คุณลักษณะและสมบัติการเร่งปฏิกิริยาของตัวเร่งปฏิกิริยาโคบอลต์บนตัวรองรับเซอร์โคเนียทรงกลมสำหรับมีเทเนชัน

นายวิทยา เหวรารักษ์

วิทยานิพนธ์นี้เป็นส่วนหนึ่งของการศึกษาตามหลักสูตรปริญญาวิศวกรรมศาสตรมหาบัณฑิต
สาขาวิชาวิศวกรรมเคมี ภาควิชาวิศวกรรมเคมี
คณะวิศวกรรมศาสตร์ จุฬาลงกรณ์มหาวิทยาลัย
ปีการศึกษา 2554
ลิขสิทธิ์ของจุฬาลงกรณ์มหาวิทยาลัย

บทคัดย่อและแฟ้มข้อมูลฉบับเต็มของวิทยานิพนธ์ตั้งแต่ปีการศึกษา 2554 ที่ให้บริการในคลังปัญญาจุฬาฯ (CUIR)
เป็นแฟ้มข้อมูลของนิสิตเจ้าของวิทยานิพนธ์ที่ส่งผ่านทางบัณฑิตวิทยาลัย
The abstract and full text of theses from the academic year 2011 in Chulalongkorn University Intellectual Repository(CUIR)
are the thesis authors' files submitted through the Graduate School.

Characteristics and catalytic properties of spherical zirconia-supported cobalt catalyst for methanation

Mr. Wittaya Hewararak

A Thesis Submitted in Partial Fulfillment of the Requirements
for the Degree of Master of Engineering Program in Chemical Engineering
Department of Chemical Engineering
Faculty of Engineering
Chulalongkorn University
Academic Year 2011
Copyright of Chulalongkorn University

Thesis Title	CHARACTERISTICS AND CATALYTIC PROPERTIES OF SPHERICAL ZIRCONIA-SUPPORTED COBALT CATALYST FOR METHANATION
By	Mr. Wittaya Hewararak
Field of Study	Chemical Engineering
Advisor	Associate Professor Bunjerd Jongsomjit, Ph.D

Accepted by the Faculty of Engineering, Chulalongkorn University in Partial Fulfillment of the Requirements for the Master's Degree

……..……..…Dean of the Faculty of Engineering
(Associate Professor Boonsom Lerdhirunwong, Dr.Ing.)

THESIS COMMITTEE

.…… Chairman
(Assistant Professor Anongnat Somwangthanaroj, Ph.D.)

……..…. Thesis Advisor
(Associate Professor Bunjerd Jongsomjit, Ph.D.)

…….. Examiner
(Assistant Professor Joongjai Panpranot, Ph.D.)

……..…….. External Examiner
(Assistant Professor Okorn Mekasuwandumrong, Ph.D.)

วิทยา เหวรารักษ์ : คุณลักษณะและสมบัติการเร่งปฏิกิริยาของตัวเร่งปฏิกิริยาโคบอลต์บนตัวรองรับเซอร์โคเนียทรงกลมสำหรับมีเทเนชัน (CHARACTERISTICS AND CATALYTIC PROPERTIES OF SPHERICAL ZIRCONIA-SUPPORTED COBALT CATALYST FOR METHANATION)
อ. ที่ปรึกษาวิทยานิพนธ์หลัก : รศ. ดร. บรรเจิด จงสมจิตร, 76 หน้า.

วิทยานิพนธ์นี้เป็นการศึกษาถึงคุณลักษณะและสมบัติการเร่งปฏิกิริยาของตัวเร่งปฏิกิริยาโคบอลต์บนตัวรองรับเซอร์โคเนียทรงกลมสำหรับกระบวนการมีเทเนชัน ซึ่งแบ่งการศึกษาออกเป็น 2 ส่วน โดยในส่วนที่ 1 เป็นการศึกษาถึงปริมาณโคบอลต์ที่แตกต่างกัน ที่ใส่ลงไปบนตัวรองรับเซอร์โคเนียทรงกลม อันได้แก่ ที่ปริมาณ 10, 15 และ 20 เปอร์เซ็นต์โดยน้ำหนัก ผลการศึกษาพบว่า ที่ปริมาณ 15 และ 20 เปอร์เซ็นต์ มีลักษณะทางกายภาพของตัวเร่งปฏิกิริยาที่คล้ายคลึงกัน ซึ่งดีกว่าที่ปริมาณ 10 เปอร์เซ็นต์ แต่ที่ปริมาณ 20 เปอร์เซ็นต์ มีอัตราการเกิดปฏิกิริยาที่สูงกว่า ทั้งนี้เนื่องจากการมีปริมาณโลหะที่ว่องไวที่พื้นผิวตัวเร่งที่สูงที่สุด นั่นคือปริมาณโลหะโคบอลต์ที่ใส่ลงไปบนตัวรองรับเซอร์โคเนียทรงกลมในปริมาณที่แตกต่างกัน มีผลที่เด่นชัดต่อคุณสมบัติการเร่งปฏิกิริยาสำหรับกระบวนการมีเทเนชัน สำหรับการศึกษาในส่วนที่ 2 เป็นการศึกษาถึงการเพิ่มประสิทธิภาพของตัวเร่งปฏิกิริยาโคบอลต์ที่มีตัวรองรับเป็นเซอร์โคเนียทรงกลม ด้วยการเติมตัว promoter คือ โลหะซีเรียม (Ce) ลงไปบนตัวรองรับ จากนั้นทำการศึกษาในส่วนของวิธีการเตรียมตัวเร่งปฏิกิริยาที่แตกต่างกันระหว่างการเตรียมโดยวิธีการเคลือบฝังแบบเป็นลำดับขั้นตอน (sequential-impregnation) ได้เป็นตัวเร่งปฏิกิริยาโคบอลต์บนตัวรองรับซีเรียม-เซอร์โคเนียทรงกลม ($Co/Ce-ZrO_2$) กับการเตรียมโดยวิธีการเคลือบฝังร่วม (co-impregnation) ได้เป็นตัวเร่งปฏิกิริยาซีเรียม-โคบอลต์บนตัวรองรับเซอร์โคเนียทรงกลม ($Ce-Co/ZrO_2$) ผลการศึกษาพบว่าตัวเร่งปฏิกิริยาที่เตรียมในทั้งสองแบบมีลักษณะทางกายภาพที่คล้ายคลึงกัน แต่ตัวเร่งปฏิกิริยาที่เตรียมแบบลำดับขั้นตอนมีอัตราการเกิดปฏิกิริยาและมีเปอร์เซ็นต์การเปลี่ยนแปลงของคาร์บอนไดออกไซด์ที่สูงกว่า ทั้งนี้เนื่องจากการมีการกระจายตัวของโลหะโคบอลต์บนตัวรองรับซีเรียม-เซอร์โคเนียที่สูงกว่าและมีบริเวณเร่งบนพื้นผิวตัวเร่งปฏิกิริยาโคบอลต์ที่สูงกว่าการเตรียมแบบฝังร่วมนั่นเอง นอกจากนี้ยังพบว่า โลหะซีเรียม มีส่วนช่วยให้ตัวเร่งปฏิกิริยาโคบอลต์บนตัวรองรับเซอร์โคเนียทรงกลมนี้มีคุณสมบัติในการรีดิวซ์ได้ง่ายขึ้น

ภาควิชา วิศวกรรมเคมี ลายมือชื่อนิสิต……..……..
สาขาวิชา วิศวกรรมเคมี ลายมือชื่อ อ.ที่ปรึกษาวิทยานิพนธ์หลัก……...……....
ปีการศึกษา 2554

##5271503621: MAJOR CHEMICAL ENGINEERING
KEYWORDS: COBALT CATALYST/ CERIUM/ ZIRCONIA/
CO_2 HYDROGENATION/ CHARACTERIZATION/ METHANATION

WITTAYA HEWARARAK: CHARACTERISTICS AND CATALYTIC PROPERTIES OF SPHERICAL ZIRCONIA-SUPPORTED COBALT CATALYST FOR METHANATION. ADVISOR: ASST. PROF. BUNJERD JONGSOMJIT, Ph.D., 76 pp.

This thesis focused on characteristics and catalytic properties of spherical zirconia-supported cobalt catalyst for methanation. The study was divided into two parts. In the first part, different amounts of cobalt were loaded on the spherical zirconia supports. The catalysts contained different Co loadings, i.e., 10 wt%, 15 wt% and 20 wt%. The results showed that the physical characteristics of 15 wt% and 20 wt% are similar which were better than those of 10 wt%. The 20 wt% of cobalt exhibited the highest reaction rate because of probably largest active metals on surface catalyst. It indicated that the amounts of different cobalt metal had distinctive effect on catalytic properties. In the second part, the study was conducted to raise the performance of spherical zirconia-supported cobalt catalyst by adding a prometer; cerium metal (Ce) onto the spherical zirconia support. This part focused on the different preparation method of cobalt catalyst between sequential-impregnation ($Co/Ce\text{-}ZrO_2$) and co-impregnation ($Co\text{-}Ce/ZrO_2$). The results showed that the physical characteristics of both catalysts are similar, but the sequential-impregnation exhibited higher reaction rate and % CO_2 conversion than the co-impregnation. This was because of the dispersion of cobalt metal on to ceria-zirconia supports and active site molecule on surface of cobalt catalyst of the sequential-impregnation were higher than that of the co-impregnation. Besides, it was found that adding cerium metal can improve reducibility of spherical zirconia-supported cobalt catalyst based on TPR study.

Department : Chemical Engineering Student's Signature ……...……..
Field of Study : Chemical Engineering Advisor's Signature ……...…….
Academic Year : 2011

ACKNOWLEDGEMENTS

This dissertation would not have been possible to complete without the support of following individuals. Firstly, He would like to express my greatest gratitude and appreciation to his advisor, Assoc. Prof. Dr. Bunjerd Jongsomjit for his invaluable guidance, providing value suggestions and his kind supervision throughout this study. In addition, he also very grateful to Assistant Professor Anongnat Somwangthanaroj, as the chairman, Assistant Professor Joongjai Panpranot and Assistant Professor Okorn Mekasuwandamrong as the members of the thesis committee for their kind cooperation.

Many thanks for kind suggestions and useful help to Mr. Jakrapan Janlamool, Miss Sasiradee Jantasee, Miss Wanna Phiwkliang, Miss Pimpatima Panupakorn, and many friends in the Research Center on Catalytic Reaction Engineering who always provide the encouragement and co-operate along the thesis study.

Finally, He would like to express his highest gratitude to my parents who always pay attention to me all the times for suggestions, support and encouragement.

CONTENTS

Page

CHAPTER

Page

CHAPTER

LIST OF TABLES

TABLE **Page**

LIST OF FIGURES

FIGURE **Page**

CHAPTER I

INTRODUCTION

Zirconia (ZrO_2) has been used extensively in work related to catalysts. It is one of the supports used widely on heterogeneous catalyst. Zirconia powder has been effectively used in different areas of chemistry, such as in ceramics and catalysis. Use of zirconia as a catalyst support has shown promising results in many environmental catalysis reactions such as CO_2 hydrogenation [Bitter, *et al*., 1997], CO oxidation [Dow, *et al*., 1994], and Fischer–Tropsch reaction [Chuah, 1999; Bruce, *et al*., 1983; Enache, *et al*., 2004]. Zirconium dioxide (zirconia, ZrO_2) has been used as a catalyst or a support. The catalytic properties of zirconia are especially promising because it has both acidic and basic properties as well as a high thermal stability. For a number of reactions, zirconia can be used as a catalyst support because of the high activity and selectivity.

Cobalt-based catalysts are applied most widely for hydrogenation reactions in a variety of systems. It has been known that supported cobalt (Co) catalysts are preferred for Fischer–Tropsch (FT) synthesis because of their high activities during FT synthesis based on natural gas, high selectivity to linear long chain hydrocarbons and also low activities for the competitive water–gas shift (WGS) reaction [Iglesia, 1997]. To increase the catalytic activity, cobalt is usually supported on a high surface area support in order to obtain a high metal dispersion. Various supports for cobalt have been used, such as silica [Panpranot, *et al.*, 2002], alumina [Panpranot, *et al.*, 2003; Das, *et al*., 2002; Zhang, *et al.*,1999], titania [Li, *et al*., 2002; Panpranot, *et al*., 2005a,b] , zeolites [Li, *et al*., 2003], zirconia [Panpranot, *et al*., 2005] and mixed alumina and zirconia [Burakorn, *et al*., 2008]. It has been shown that the reducibility of the cobalt catalysts and, in general, the dispersion of the metal phase formed depends on the support [Kraum, and Baerns, 1999], the cobalt precursor [Kraum, and Baerns, 1999; Sun, *et al*., 2000], the metal loading [Riva, *et al*., 2000], the preparation method, thermal treatment and the reduction process [Zhang, *et al.*, 1999]. Besides,

modification of the supports would also has influence on the significant change in the characteristics and reaction behaviors of the catalysts.

Cobalt perovskites show good catalytic activity for the total oxidation of methane [Milt, *et al*., 1996; Ferri, *et al*., 1998; Connell, *et al*., 1999], but the surface areas are low. In order to increase the surface areas, these active oxides should be supported on high surface area solid [Milt, *et al*., 2001].

For preparation of zirconia-supported cobalt catalyst, the incipient wetness impregnation method is commonly used for preparation of supported metal catalysts due to its simplicity and the possibility for preparation in large quantity. The zirconia prepared in 1,4-butanediol as the support resulted in the high surface acidity consequently having the high activity and show high surface area [Wongmaneenil, *et al*., 2010]. For CO_2 hydrogenation reaction, this reaction will convert carbon dioxide into carbon monoxide (CO) and oxygen (O_2) caused by the instability of carbon monoxide gas. Then, it will continuously react to the atomic hydrogen into hydrocarbons.

Besides, it has been discovered that some rare earth oxides like La_2O_3 and CeO_2 exert an influence on CO hydrogenation over supported metal catalysts [Pierantozzi, 1985; Barrault, *et al*., 1986; Zhou, *et al*., 1991 ; Guerrero-Ruiz, *et al*., 1994]. For instance, lanthanum or cerium oxide promoters are reported to improve the total activity and increase the selectivity to alkenes and higher hydrocarbons of carbon-supported Co and Ru catalysts [Barrault, *et al*., 1986]. Ceria stabilized zirconia has attracted attention in recent years due not only to its good mechanical and electrical properties, but also to its application as catalysts, given their good stability and redox properties. However, the properties of these materials largely depend on the preparation method, the nature of the present phases and their contents. It has been shown that phase segregation of binary oxides could be suppressed by doping with proper elements. The substitution of zirconium atoms by iron ones can generate oxygen vacancies in the tetragonal network of ZrO_2–CeO_2 system prepared by the solid-state route, or phase segregation could be inhibited by doping the mixed oxide with rare earth elements [Mastelaro, *et al*., 2003; Aneggi, *et al*., 2006].

As mentioned above, base on the properties of zirconia, cobalt catalyst, cerium catalyst and catalyst preparation process, it is the origin of this research that points to the support of the zirconia in a spherical shape prepared by solvothermal method using 1,4-butanediol as solvent. The scope of the study was divided into three parts, where in the first part, different amounts of cobalt loaded onto the zirconia support were investigated for activity and selectivity of CO/H_2O catalyst via CO_2 hydrogenation. In the second part, the addition of the promoter such as cerium onto zirconia support by using the method of preparation is sequential-impregnation was investigated. In the third part, the method of preparation is co-impregnation was performed.

In this research, it was focused on the characteristics and catalytic properties of spherical zirconia-supported cobalt catalyst. The study divided into two parts. In part 1, for study in term of a different amount cobalt are loaded on the spherical zirconia supports. The catalysts having different Co loadings, i.e., 10 wt%, 15 wt% and 20 wt%. In second part is study to raise performance of spherical zirconia-supported cobalt catalyst. By adding a prometer is cerium metal (Ce) on to the spherical zirconia support. In this part are focused in the differential preparation of cobalt catalyst between sequential-impregnation ($Co/Ce\text{-}ZrO_2$). and co-impregnation ($Co\text{-}Ce/ZrO_2$). The characteristics and catalytic properties were analyzed by means of X-ray diffraction (XRD), scanning electron microscopy (SEM), energy dispersive X-ray analysis (EDX), N_2-physisiprtipn (BET), temperature-programmed reduction (TPR) and carbon monoxide (CO) chemisorptions. The reaction study on carbon dioxide (CO_2) hydrogenation under methanation was performed in order to evaluate the catalytic activity and selectivity of products.

1.1 The study was scoped as follows:

Part 1: Study of Co/ZrO_2 catalysts

1. Preparation of the spherical nanocrystalline zirconia support (mesoporous meterial) by solvothermal method.
2. Characterization of the zirconia support using scanning electron microscopy (SEM), X-ray diffraction (XRD) and N_2-physisorption (BET).
3. Preparation of the spherical nanocrystalline zirconia-supported cobalt catalyst using the incipient wetness impregnation method by varying different cobalt loading, i.e., 10 wt%, 15 wt% and 20wt%.
4. Characterization of the catalyst using scanning electron microscopy (SEM), N_2-physisorption (BET), X-ray diffraction (XRD), temperature-programmed reduction (TPR), carbon monoxide (CO) chemisorptions.
5. Reaction study of the catalyst samples in carbon dioxide (CO_2) hydrogenation at 220^oC and 1 atm and a H_2/CO ratio of 10 under methanation condition in a middle of fixed-bed micro reactor.

Part 2: Study of modified $Ce\text{-}ZrO_2$-supported Co catalysts**,**
by sequential-impregnation method
(Cobalt was loaded after cerium was modified)

1. Preparation of the spherical nanocrystalline zirconia support (mesoporous meterial) by solvothermal method.
2. Characterization of the zirconia support using scanning electron microscopy (SEM).
3. Preparation of modified-spherical ZrO_2 supports with 5 wt% Ce using the incipient wetness impregnation method.
4. Characterization of the modified $Ce\text{-}ZrO_2$ supports using scanning electron microscopy (SEM), energy dispersive X-ray analysis (EDX), X-ray diffraction (XRD) and N_2-physisorption (BET).

5. Preparation of the Ce-ZrO_2-supported cobalt catalyst (15 wt% Co) using the incipient wetness impregnation method.
6. Characterization of the catalyst using scanning electron microscopy (SEM), energy dispersive X-ray analysis (EDX), N_2-physisorption (BET), X-ray diffraction (XRD), temperature-programmed reduction (TPR), carbon monoxide (CO) chemisorptions.
7. Reaction study of the catalyst samples in carbon dioxide (CO_2) hydrogenation at 220^oC and 1 atm and a H_2/CO ratio of 10 under methanation condition in a middle of fixed-bed micro reactor.

Part 3: Study of modified Co-Ce/ZrO_2 catalysts**,**
by co-impregnation method
(cerium and cobalt were loaded together)

1. Preparation of the spherical nanocrystalline zirconia support (mesoporous meterial) by solvothermal method.
2. Characterization of the zirconia support using scanning electron microscopy (SEM).
3. Preparation of the modified-spherical zirconia supported cobalt catalyst with 15 wt% Co and 5% wt% Ce using the incipient wetness co-impregnation method.
4. Characterization of the catalyst using scanning electron microscopy (SEM), energy dispersive X-ray analysis (EDX), N_2-physisorption (BET), X-ray diffraction (XRD), temperature-programmed reduction (TPR), carbon monoxide (CO) chemisorptions.
5. Reaction study of the catalyst samples in carbon dioxide (CO_2) hydrogenation at and 1 atm and a H_2/CO ratio of 10 under methanation condition in a middle of fixed-bed micro reactor.

CHAPTER II

LITERATURE REVIEWS

There are several studies of cobalt catalyst, zirconia-supported, cerium oxide promoters and catalyst for CO_2 hydrogenation reaction. Many researchers have found the useful knowledge about this research especially the zirconia-supported cobalt catalyst in CO_2 hydrogenation. These reports are very useful and will use to develop works for the future.

2.1 Zirconia Support

Supports have significant effect on catalytic activity and stability with carbon dioxide reforming of methane (dry reforming) [Nagaoka, *et al*., 2001; Wang, *et al*., 2000]. The use of ZrO_2 can result in attractive process benefits owing to its redox behavior, surface acidity, reducibility and high thermal stability. [Özkara-Aydınoğlu, *et al*., 2009; Stagg-Williams, *et al*., 2000; Mattos, *et al*., 2003] have shown that the addition of Ce and La to the ZrO_2 support resulted in significant improvement in the stability, with no decrease in both CH_4 and CO_2 conversions.

Wongmaneenil *et al*. [2010] studied solvent effect on synthesis of zirconia support for tungstated zirconia catalysts (WO_x/ZrO_2 (WZ)). The solvothermal reaction of zirconium n-butoxide (ZNB) in different solvent media, such as 1,3-pentanediol, 1,4-butanediol, 1,5-pentanediol and 1,6-hexanediol resulted in the formation of zirconium dioxide (ZrO_2) nanostructure. Then, the 15%W/ZrO_2 (WZ) catalysts using different zirconia supports were prepared by impregnation method. The effects of solvent on preparation of zirconia on the catalytic performance of WZ catalysts in esterification of acetic acid and methanol at 60 ^{0}C were investigated. The experimental results showed that ZrO_2 particles prepared in 1,4-butanediol (ZrO_2-BG) have a spherical shape, while in other glycols the samples were irregularly-shaped particles. The reaction results of esterification illustrated that the W/ZrO_2-BG catalysts had high surface acidity and showed high acetic acid conversion. The W/ZrO_2-PeG catalysts (ZrO_2 particles prepared in 1,5-pentanediol, PeG) exhibited the

lowest surface acidity among other samples due to strong interaction of proton species and the zirconia supports as proven by TGA. One of the possible reasons can be attributed to different amounts of carbon residue on the surface of catalysts. This study revealed the effects of solvent on morphology and other characteristics of zirconia and their performance as tungstated zirconia catalyst. It was found that a series of WO_x/ZrO_2 catalysts exhibited the tungsten density in the range of 3.9 to10.0 W-atoms/nm^2. XRD and Raman spectroscopy results indicated that the W phase is present as a surface interaction species. No evidence for the formation of WO_3 was found. The zirconia prepared in 1,4-butanediol as the support resulted in the highest surface acidity consequently having the highest activity. The lower activities of tungstated zirconia catalysts prepared in other solvents were due to stronger interaction of proton species and the zirconia supports as shown by weight losses of samples in the TGA profiles. The type of solvent used for preparation of the glycothermal-derived zirconia may affect the amount of carbon residue and WO_x monotungstate/polytungstate ratio on the surface of catalysts resulting in the difference in proton species-support interaction behavior.

Khaodee *et al*. [2008] studied the effect of temperature ramping rate during calcinations on characteristics of nanoscale zirconia and its catalytic activity for isosynthesis. The heating rate of calcinations was varied in the range of 1.0-10.0 ^{0}C/min. They found that a composition of the tetragonal phase of zirconia increases with the increased temperature ramping rate during calcination, but it insignificant influence on the other physical properties such as BET surface area, cumulative pore volume and pore diameter. The intensity of Zr^{3+} on the surface varied with the change in the heating rate of calcination. Both the tetragonal phase composition in zirconia and the quantity of Zr^{3+} were the key factors affecting the selectivity to isobutene in hydrocarbons. For the catalytic activity, the acid sites did not affect the activity, but the basic sites depended on the fraction of the tetragonal phase in zirconia which was related to the selectivity to isobutene.

2.2 Ceria-Zirconia Oxides

Aguiar *et al*. [2002] found that cerium oxide (CeO_2) and ceria-zirconia (CeO_2-ZrO_2) are useful in a wide variety of applications involving oxidation or partial oxidation of hydrocarbons (e.g. automotive catalysis) and as components of anodes for SOFCs. This material has high oxygen storage capacity, which is beneficial in oxidation processes and carbon combustion. The excellent resistance toward carbon formation from methane cracking reaction over CeO_2 compared to commercial Ni/Al_2O_3 was also reported recently**.**

The addition of zirconium oxide (ZrO_2) to cerium oxide (CeO_2) has been found to improve the oxygen storage capacity, redox property, thermal stability, and catalytic activity**.**

Damyanova *et al*. [2008] studied the surface and redox properties of ceria–zirconia oxides**.** CeO_2–ZrO_2 oxides with different CeO_2 content (1–12 wt%) were prepared by the impregnation method. Spectroscopic data showed that the tetragonal phase of zirconia is preserved in all CeO_2–ZrO_2 oxides, although they retain a high number of defect sites caused by a strong interaction between zirconia and cerium oxide species. An enrichment of the zirconia surface with a fluorite structure of CeO_2 is observed for the CeO_2– ZrO_2 oxide with the highest CeO_2 content (12 wt%). The samples subjected to consecutive reduction–oxidation cycles at different temperatures showed good redox properties related to the increase of oxygen mobility. It was concluded that these CeO_2–ZrO_2 oxide systems, displaying high surface and good thermal stability, are similar to chemically mixed oxides due to the strong interaction between the zirconia carrier and deposited ceria.

2.3 Zirconia-Supported Cobalt Catalysts

Panpranot *et al*. [2005] studied the differences in characteristics and catalytic properties of Co catalysts supported on micron- and nano-sized zirconia. Nanocrystalline zirconia was prepared by decomposition of zirconium tetra n-propoxide in 1,4-butanediol and was employed as a support for cobalt catalysts. The

activity and the selectivity of the catalyst in CO hydrogenation were compared with cobalt supported on commercial available micron- and nano-sized zirconia. The catalytic activities were found to be in the order: Co/ZrO_2-nano-glycol >> Co/ZrO_2-nano-com > Co/ZrO_2-micron-com. Compared to the micron-sized zirconia supported one, the use of commercial nano-sized zirconia resulted in higher CO hydrogenation activity but lower selectivity for longer chain hydrocarbons (C_4-C_6), whereas the use of glycothermal-derived nanocrystalline zirconia exhibited both higher activity and selectivity for C_4-C_6. The better performance of the latter catalyst can be ascribed to not only the effect of the presence of pure tetragonal phase of zirconia. The glycothermal-derived catalysts exhibited higher surface areas, higher Co dispersion, and highly stable pure tetragonal phase zirconia.

Özkara-Aydınoğlu *et al*. [2010] studied carbon dioxide reforming of methane (dry reforming) over Co/ZrO_2 catalysts promoted with different metal additives (La, Ce, Mn, Mg, K) aiming to improve the performance of the catalysts and increase their resistance to coking. Scanning electron microscopy studies and different activity levels of the catalysts clearly show that the type of the promoter significantly affected the metal dispersion properties and catalytic performances of Co/ZrO_2 catalysts. La-modified catalyst exhibited high stability, but moderate activity. It showed no severe coke deposition. Ce-doped Co/ZrO_2 displayed the highest activity among all the catalysts prepared and had a very limited activity loss. The type of the metal additive used significantly affected the metal dispersion properties and catalytic performances of promoted-Co/ZrO_2 catalysts. Monometallic Co/ZrO_2 had high initial activity but it suffered from severe carbon deposition. La-modified catalyst exhibited high stability, but moderate activity. It showed no severe coke deposition. Ce doped Co/ZrO_2 displayed the highest activity among all the catalysts prepared and had a very limited activity loss in time-on-stream tests. The different activity levels of the catalysts clearly show that the catalytic performance of promoted-Co/ZrO2 samples strongly depends on the type of the metal additive used. The observed order of methane conversions over doped cobalt catalysts in terms of the type of promoters added is Ce > none > La ≈ Mn > K > Mg for the reaction performed 6 hours of times-on-stream (TOS).

2.4 Supported Cobalt Catalysts

Supported cobalt catalysts are important for the Fischer–Tropsch synthesis of high molecular weight, paraffinic waxes which can be hydrocracked to produce lubricants and diesel fuels. The type and structure of the support influence the dispersion, particle size and reducibility, and thereby the activity for Co-supported catalysts. Beside the support, the promoter is one important focuses in the development of this process is the improvement of the catalyst activity by increasing the number of active Co metal sites that are stable under reaction conditions.

Ali *et al*. [1995] investigated the influence of Zr promotion of 20 wt% Co/SiO_2 on Fischer-Tropsch synthesis using catalysts prepared in different ways and having different loadings of Zr (up to 8.5 wt%). The Zr-promoted exhibited higher overall rates of FTS compared to unpromoted Co/SiO_2. The sequentially impregnated $Co/Zr/SiO_2$ catalysts appeared to be the most active. However, the co-impregnation method of preparation appeared to result in higher cobalt dispersion. While Zr promotion did not appear to promote or inhibit H_2 activation, hydrogen spillover may have been partly responsible for enhancing the activity of the sequentially impregnated $Zr/Co/SiO_2$ catalysts. Zr also possibly created an active interface with Co that increased catalyst activity by facilitating Co dissociation. Although high levels of promotion tended to increase the selectivity for higher hydrocarbon, Zr appears to be primarily an excellent rate promoter for Co/SiO_2. Similarly,

Fröhlich *et al*. [1996] studied activation and deactivation of Co foils during hydrogenation of carbon dioxide in dependence on pretreatment of the catalyst and time on stream, temperature and composition of the educt gas. Modifications of the surface due to activation and deactivation have been investigated by means of a combination of various methods, including temperature programmed processes as well as Auger electron spectroscopy and electron microscopy. Both oxidation/ reduction of the surface and incorporation of oxygen and carbon in the bulk lead to marked changes in the surface structure and a considerable increase in surface area. The catalytic activity of the oxidized surface concerning the hydrogenation of CO_2 is small, but increases strongly with reduction. Deactivation is accompanied with

structural changes and proved to be reversible. Chemical poisoning was only observed after addition of hydrogen sulfide to the educt gas. Two types of reactors have been used, a plug-flow reactor and a batch reactor. The influences of pretreatment of the catalyst, reaction temperature, composition of the educt gas and change in temperature during the reaction on the composition of the product gas as well as on the dependence of the rate of reaction on TOS were investigated.

Repeated reduction/oxidation cycles increase the activity of the cobalt foils in regard to all the products (methane, ethane, propane and carbon monoxide). There is a strong influence of reaction temperature on both activation of the catalyst, which was installed in oxidized state and the rates of the catalytic reactions.

Deactivation, that is observed during the isothermal reaction, reduces the rate of formation of hydrocarbons more than that of formation of carbon monoxide. It is a reversible deactivation, i.e., the catalyst can easily be reactivated by a simple reduction/oxidation cycle. Concerning the deactivation the same occurs during temperature programmed reactions: When a distinct temperature is exceeded the rate of reaction strongly decreases and finally approaches zero. The maximum rate is observed at temperatures which increase in the sequence propane, ethane, methane, carbon monoxide.

The preliminary activation of the catalyst occurs not only via pre-oxidation of the cobalt surface but can be increased by reduction/oxidation cycles which lead to an increase or a roughening of the surface region. It has been found that from one reduction/oxidation cycle to the following cycle, during oxidation, oxygen can continuously penetrate deeper into the bulk. This process contributes to the observed roughening of the surface region. Only surface oxygen can be completely removed from the surface by hydrogenation. This reaction is fast.

The oxidized surface is not active in the hydrogenation reaction, activation occurs within the first few minutes of the reaction.

The deactivation discussed so far, is traced back to structural changes in the surface of the catalyst. There is evidence that deactivation is not only caused by a decrease in the surface area. It is likely that also qualitative changes take place, which affect the formation of the various products in different extent. Chemical poisoning of the catalyst could only be observed in the case of hydrogen sulfide added to the educt gas. Interruption of the catalytic reaction by exposure of the catalyst to a continuous

flow of nitrogen had almost no influence, oxygen led to considerable reactivation and hydrogen to pronounced sintering of the surface.

Feller *et al*. [1999] studied the addition of zirconium oxide chloride to the catalyst formulation of Co/SiO_2. It leads to a higher reducibility of cobalt, due to the formation of a cobalt zirconium species, which can be reduced at lower temperatures than cobalt silicate. Furthermore, the metal particle size of cobalt is increased, but the size of cobalt clusters is reduced. The $Co–Zr/SiO_2$ catalysts were tested for their activity in the Fischer–Tropsch synthesis. The steady-state activity increased with increasing zirconium loading, which was attributed to the resistance against reoxidation of the larger cobalt particles and thus to the larger amount of surface cobalt metal present at steady-state in the zirconium promote catalysts. With increasing zirconium content the number of surface metal atoms at steady-state conditions increases, leading to a higher extent of secondary reactions, but the size of the cobalt clusters decreases, leading to a decrease in the extent of secondary reactions. With increasing zirconium content the extent of secondary hydrogenation of olefins (e.g., ethene) passes a minimum, and the C_5^+ selectivity passes a maximum due to readsorption of small, reactive organic product compounds, which can be incorporated in larger product compounds. Double bond isomerization increases with increasing zirconium content. This might be attributed to the catalytic activity of zirconia

Burakorn *et al*. [2008] studied the physicochemical properties of cobalt (Co) as a catalytic phase for carbon monoxide (CO) hydrogenation reaction, dispersed on mixed nano-$Al_2O_3–ZrO_2$ supports. The samples of nano-$Al_2O_3–ZrO_2$ supports were prepared by the solution mixing which consisting of various weight ratios [0–100 wt%] of nano-ZrO_2 and the 20wt% of cobalt were dispersed loading on the mixed nano-$Al_2O_3–ZrO_2$ support by the incipient wetness impregnation. After calcination, the samples were characterized with different techniques. XRD revealed that the Co_3O_4 oxide species were detected on various supports without changes in morphologies. There was no significant change in morphologies and elemental distributions of samples as seen from SEM/EDX. The presence of ZrO_2 in the mixed supports could result in the low number of active Co metal atoms as detected using H_2

chemisorption due to a strong support interaction. This resulted in lower activity of the sample. However, the chain growth probability was found to increase with the presence of the nano-ZrO_2 in the mixed nano-Al_2O_3–ZrO_2 support. For CO hydrogenation study, the Co dispersed on the nano-Al_2O_3 was the most active among any other samples. However, the Co dispersed on the mixed nano-Al_2O_3–ZrO_2 apparently resulted in longer chain hydrocarbons produced.

2.5 The supported metal catalysts (Promoted) in CO and CO_2 hydrogenation system

The catalytic hydrogenation of carbon monoxide and carbon dioxide produces a large variety of products ranging from methane and methanol to higher molecular weight alkanes, alkenes and alcohols.

Chen *et al*. [1997] studied CO hydrogenation over zirconia supported iron catalysts promoted with rare earth oxides such as La_2O_3 and CeO_2, which prepared by sequential impregnation method. It is shown that the structure, reduction behavior, and the catalytic property for CO hydrogenation of these catalysts are quite different from that of the unpromoted Fe/ZrO_2 sample, and are influenced significantly by the kinds of promoter elements. For the Fe/La/ZrO_2 sample, the catalytic activity is only a little bit higher than that of the Fe/ZrO_2 sample, but light olefins selectivity increases and methane formation is suppressed. For the Fe/Ce/ZrO_2 sample, the catalytic activity is much higher than that of the unpromoted Fe/ZrO_2 sample, while methane formation is suppressed and light olefins selectivity slightly increases. In part of the role of different rare earth oxide promoters in these catalysts, For the Fe/La/ZrO_2 sample, Fe_2O_3 particles highly disperse on the La_2O_3 layer, reduction of iron oxide becomes difficult owing to the strong interactions between iron oxide and La_2O_3. The catalytic activity is only a little bit higher than that of the Fe/ZrO_2 sample, but light olefins selectivity increases and methane formation is suppressed. The promotion effect of lanthanum can be attributed to the basic character and the electronic effect of lanthana layer, which increases the electron density of the iron particles and enhances the dissociation of CO. For the Fe/Ce/ZrO_2 sample, dispersion of iron oxide decreases by the addition of CeO_2 layer. The catalytic activity is much higher than that of the

unpromoted Fe/ZrO_2 sample, while methane formation is suppressed and light olefins selectivity slightly increases. The promotion effect of ceria can be explained in terms of the formation of new catalytic active sites (Fe-CeO_2 ensembles) at which the CO may bond with its carbon atom to iron atom and its oxygen atom to the adjacent partially reduced cerium oxide. This arrangement results in a weakening of the C-O bond, and the dissociation and reaction of CO is markedly enhanced.

Pérez-Alonso *et al*. [2008] were investigated the carbon dioxide hydrogenation over Fe-Ce catalyst. Unpormoted and Ce-pormoted Fe catalysts have been tested. Under the selected reaction conditions (573 K, 1.01 MPa, H2/CO = 3, GHSV = 15.5 L h^{-1} g^{-1} cat), the results show that both materials are similar catalytic performance, reaching similar conversion levels and yielding hydrocarbons (C_1–C_{10}) with high selectivity. The chain growth probability (α) obtained is very similar in both cases (0.44). Although Ce incorporation into the base iron catalyst does not modify the CO_2 hydrogenation performance, the promoter addition shortens the time required to reach stationary-state operation in a great extent (from 70 to 30 h).

Lahtinen *et al*. [1994] investigated C, CO and CO_2 hydrogenation on cobalt foil model catalysts. They were found that the reactions produce mainly methane, but with selectivity of 98, 80, and 99 wt% at 525 K for C, CO and CO_2, respectively. The rate of methane formation on cobalt foil shows zero order partial pressure dependence on CO_2 and first order partial pressure dependence on H_2. The reaction proceeds via dissociation of C-O bonds and formation of CoO on the surface. The reduction of CoO is the rate limiting step in the CO and CO_2 hydrogenation reaction. These authors also proposed the reaction mechanisms for C, CO and CO_2 hydrogenation.

Table.2.1 The reaction mechanisms proposed for C, CO and CO_2 hydrogenation.

C Hydrogenation	CO Hydrogenation	CO_2 Hydrogenation	
	$CO^{+}* <-> CO*$	$CO_2^{+}* <-> CO_2*$	
$H_2^{+2}* <-> 2H^{+}$	$H_2^{+2}* <-> 2H^{+}$	$H_2^{+2}* <-> 2H^{+}$	
		$CO_2* + Co <-> CO* + CoO$	
	$CO* + Co <-> C* + CoO$	$CO* + Co <-> C* + CoO$	$CO* + H* <-> COH*+*$
$C* + H* <-> CH*+*$	$C* + H* <-> CH*+*$	$C* + H* <-> CH*+*$	or $COH* + H* <-> H_2CO*+*$
$CH* + H* <-> CH_2*+*$		$CH* + H* <-> CH_2*+*$	$HCO* + Co <-> CH_2* + CoO$
$CH* + H* <-> CH_3*$	$CH_2* + H* <-> CH_3*$	$CH_2* + H* <-> CH_3*$	
$CH_3* + H* <-> CH_4^{+2}*$	$CH_3* + H* <-> CH_4^{+2}*$	$CH_3* + H* <-> CH_4^{+2}*$	
	$CoO + H* \rightarrow OH* + Co$	$CoO + H* \rightarrow OH* + Co$	
	$OH* + H* <-> H_2O^{+2}*$	$OH* + H* <-> H_2O^{+2}*$	

CHAPTER III

THEORY

3.1 Cobalt oxide

Cobalt has three well-known oxides:

Cobalt (II) oxide, CoO, is an olive green, cubic crystalline material. Cobalt (II) oxide is the final product formed when the carbonate or the other oxides are calcined to a sufficiently high temperature, preferably in a neutral or slightly reducing atmosphere. Pure cobalt (II) oxide is a difficult substance to prepare, since it readily takes up oxygen even at room temperature to re-form a higher oxide. Above about 850^{o}C, cobalt (II) oxide form is the stable oxide. The product of commerce is usually dark gray and contains 75-78 wt % cobalt. Cobalt (II) oxide is soluble in water, ammonia solution, and organic solvents, but dissolves in strong mineral acids. It is used in glass decorating and coloring and is a precursor for the production of cobalt chemical.

Cobalt (III) oxide, Co_2O_3, is formed when cobalt compounds are heated at a low temperature in the presence of an excess of air. Some authorities told that cobalt (III) oxide exists only in the hydrate form. The lower hydrate may be made as a black power by oxidizing neutral cobalt solutions with substances like sodium hypochlorite. Co_2O_3 or $Co_2O_3 \cdot H_2O$ is completely converted to Co_3O_4 at temperatures above 265^{o}C. Co_3O_4 will absorb oxygen in a sufficient quantity to correspond to the higher oxide Co_2O_3.

Cobalt oxide, Co_3O_4, is formed when cobalt compounds, such as the carbonate or the hydrated sesquioxide, are heated in air at temperatures above approximately 265^{o}C and not exceeding 800^{o}C.

3.2 Zirconia

Zirconia, zirconium dioxide, an industrially important compound of zirconium and oxygen usually derived from the mineral zircon.

Zirconia ceramics is a ceramic material consisting of at least 90% of Zirconium Dioxide (ZrO_2).

Zirconium Oxide is produced from natural minerals such as Baddeleyite (zirconium oxide) or zirconium silicate sand.

Pure zirconia changes its crystal structure depending on the temperature:

At temperatures below 2138ºF (1170ºC) zirconia exists in monoclinic form. At the temperature 2138ºF (1170ºC) monoclinic structure transforms to tetragonal form which is stable up to 4300ºF (2370ºC). Tetragonal crystal structure transforms to cubic structure at 4300ºF (2370ºC). Structure transformations are accompanied by volume changes which may cause cracking if cooling/heating is rapid and non-uniform.

Additions of some oxides (MgO, CaO, Y_2O_3) to pure zirconia depress allotropic transformations (crystal structure changes) and allow to stabilize either cubic or tetragonal structure of the material at any temperature. The most popular stabilizing addition to zirconia is yttria (Y_2O_3), which is added and uniformly distributed in proportion of 5.15%.

Depending on sintering temperature and other processing parameters, the following forms of stabilized zirconia may be prepared:

1. Fully stabilized zirconia (FSZ) with cubic crystal structure;
2. Partially stabilized zirconia (PSZ) with mixed structure (cubic+tetragonal);
3. Polycrystalline tetragonal zirconia (TZP) with metastable tetragonal structure of very fine zirconia grains sintered at low temperature.

3.3 Cerium oxide

Cerium oxide is widely employed as a promoter for supported-noble metal catalysts due to its advantages:

- To stabilize the metal dispersion on the carrier;
- To improve the oxidation and reduction of the noble metal;
- To enhance oxygen storage and release by shifting between CeO_2 under reducing conditions, respectively

However, the major problem of CeO_2 when used as a carrier is the loss of oxygen storage capacity (OSC) due to a reduction in surface area upon thermal treatment. Insertion of zirconia into the cubic CeO_2 framework with formation of a solid solution results in increased thermal stability and improved redox properties due to the high efficiency of the Ce^{4+}, Ce^{3+} redox cycle [M. Pijorat *et al*., 1995; P. Fornasiero *et al*., 1996; R. Di Monte *et al*., 2000].

Cerium metal tarnishes slowly in air and burns readily at 150 °C to form cerium (IV) oxide:

$$Ce + O_2 \rightarrow CeO_2$$

3.4 Hydrogenation Reaction

Hydrogenation is a chemical reaction in which hydrogen atoms add to carbon-carbon multiple bonds. In order for the reaction to proceed at a practical rate, a catalyst is almost always needed. Hydrogenation reactions are used in many industrial processes as well as in the research laboratory, and occur also in living systems.

For CO_2 hydrogenation reaction, this reaction will convert carbon dioxide into carbon monoxide (CO) and oxygen (O_2) caused by the instability of carbon monoxide gas. Then, it will continuously react to the atomic hydrogen into hydrocarbons. CO_2 is converted to light hydrocarbon such as methane (CH_4), ethane (C_2H_6), propane (C_3H_8), etc.

Efficient heterogeneous catalysts have been developed for synthesis of

- Methanol, Ethanol
- Dimethyl ether
- CH_4 and higher hydrocarbon
- Formic acid
- Dimethylformamide

3.5 Methanation

Methanation is a physical-chemical process to generate methane from a mixture of various gases out of biomass fermentation or thermo-chemical gasification. The main components are carbon monoxide and hydrogen.

The following main process describes the methanation:

$$CO + 3\ H_2 \rightarrow CH_4 + H_2O$$

This process is used for the generation of biogenous natural gas substitute, which can be fed into the gas grid**.**

Methanation is the reverse reaction of steam methane reforming, which converts methane into synthesis gas.

Methanation is the removal of carbon monoxide and carbon dioxide that mixed in the gas mixture is about 0.3% and 0.5%, respectively, into methane. In the equation.

$$CO + 3\ H_2 \rightarrow CH_4 + H_2O$$

$$CO_2 + 4H_2 \rightarrow CH_4 + 2H_2O$$

The reason of elimination the carbon monoxide or carbon dioxide gas in gas mixture because the severity of it, if there is such a little gas. It will react with the iron. As a catalyst in the synthesis of ammonia, causing the catalyst deactivation. But methane does not cause such adverse effects synthesis of ammonia, causing the catalyst deactivation. But methane does not cause such adverse effects.

CHAPTER IV

EXPERIMENTAL

This chapter consists of experimental systems and procedures used in this work which is divided into three parts including catalyst preparation, catalyst characterization and reaction study in CO_2 hydrogenation.

The first part (section 4.1) is described spherical zirconia support preparation and preparation of Co catalyst. The second part (section 4.2) is explained catalyst characterization by various techniques including of N_2 physisorption (BET), TPR, XRD, SEM, and CO Chemisorptions. Finally, the last part (section 4.3) is illustrated catalyst activity measurement in CO_2 hydrogenation.

4.1 Catalyst preparation

4.1.1 Chemicals

The details of chemicals used in this experiment are shown in Table 4.1

Table 4.1 Chemicals used in the preparation of catalysts.

Chemical	Supplier
Cobalt (II) nitrate hexahydrate 98% ($Co(NO_3)_2 \cdot 6H_2O$)	Aldrich
Zirconium tetra-n-butoxide 80 wt% solution in 1-butanol (ZNB)	Aldrich
1,4-butanediol (purity 99%)	Sigma–Aldrich
Cerium (III) nitrate hexahydrate ($Ce(NO_3)_3 \cdot 6H_2O$)	Aldrich

4.1.2 Preparation of spherical zirconia supported, ZrO_2

Zirconium dioxide was prepared by solvothermal reaction. Approximately, 35 g of zirconium tetra-n-butoxide 80 wt% solution in 1-butanol (ZNB, Aldrich) was suspended in 100 ml of the desired solvent in a test tube, which was then placed in a 300 ml autoclave. The solvent used in this work was 1,4-butanediol (purity 99%, Sigma–Aldrich). The gap between autoclave wall and the test tube was filled with 30 ml of the same solvent. The autoclave was completely sealed and purged with nitrogen. The mixture was heated to 300^0C at a heating rate of 2.5^0C/min and kept at that temperature for 2 h. After cooling to room temperature, the resulting powders were collected after repeated washing with methanol by centrifugation. The products were then air-dried at 110^0C for 12 h and calcined at 450^0C for 3 h at a heating rate of 10^0C/min.

4.1.3 Preparation of the modified-zirconia support

A modified-zirconia support was prepared by the incipient wetness impregnation. A Cerium (III) nitrate hexahydrate [$(Ce(NO_3)_3 \cdot 6H_2O$] (5 wt% loading) was dissolved in de-ionized water which its volume equals to pore volume of catalyst and then impregnated on to prepared zirconia. The Ce solution was dropped slowly to the zirconia support. The modified-zirconia was dried at 110^0C for 12 h and calcined in air at 450^0C for 3 h at a heating rate of 10^0C/min.

4.1.4 Preparation of Co catalyst

The zirconia samples obtained from 4.1.2 were used as supports. The zirconia supports loaded with cobalt were prepared by the incipient wetness impregnation method using cobalt (II) nitrate hexahydrate [$Co(NO_3)_2 \cdot 6H_2O$] as a precursor onto the obtained spherical zirconia sufficient for different yield materials as 10, 15 and 20 wt% of CO loading. The catalysts were dried at

110^0C for 12 h and calcined in air at 450^0C for 3 h at a heating rate of 10^0C/min.

The zirconia samples obtained from 4.1.3 were used as modified zirconia supports (the sequential-impregnation method). The modified zirconia supports loaded with cobalt were prepared by the incipient wetness impregnation method using cobalt (II) nitrate hexahydrate [$Co(NO_3)_2$•$6H_2O$] as a precursor onto the obtained spherical zirconia sufficient for 15 wt% of CO loading. The catalysts were dried at 110^0C for 12 h and calcined in air at 450^0C for 3 h at a heating rate of 10^0C/min.

The zirconia samples obtained from 4.1.2 testing in step 3 were used as modified zirconia supported cobalt catalyst. The zirconia supports loaded with cobalt and cerium were prepared by the incipient wetness impregnation method (co-impregnation method) using cobalt (II) nitrate hexahydrate [$Co(NO_3)_2$•$6H_2O$] and Cerium (III) nitrate hexahydrate [($Ce(NO_3)_3$•$6H_2O$] as together precursor onto the obtained spherical zirconia sufficient for 15 wt% of CO loading and 5 wt% of Ce loading. The catalysts were dried at 110^0C for 12 h and calcined in air at 450^0C for 3 h at a heating rate of 10^0C/min.

4.2 Catalyst Characterization

4.2.1 X-Ray Diffraction (XRD)

XRD was performed to determine the bulk crystalline phases and crystalline size of various investigated catalyst samples. It was conducted using a SIEMENS D-5000 X-ray diffractometer connected with a computer with Diffract ZT version 3.3 program for fully control of the XRD analyzer. The experiments were carried out by using Cu K_α (λ = 1.54439 Å) radiation with Ni filter. The spectra were scanned at a rate of 2.4 degrees/min in the range 2θ of 20-80 degrees resolution 0.04^o. The crystallite size was estimated from line broadening according to the Scherrer equation and α-Al_2O_3 was used as a standard.

4.2.2 N_2 Physisorption (BET)

BET surface area, pore volume and pore diameter were measured by N_2 adsorption–desorption isotherm at liquid nitrogen temperature (-196 ˚C) using a Micromeritics ASAP 2020. The surface area and pore distribution were calculated according to Brunauer-Emmett-Teller (BET) and Barret-Joyner-Halenda (BJH) methods, consecutively.

The reaction apparatus of BET surface area measurement consisted of two feed lines for helium and nitrogen. The flow rate of the gas was adjusted by means of fine-metering valve on the gas chromatograph. The sample cell made from pyrex glass. The mixture gases of helium and nitrogen flowed through the system at the nitrogen relative of 0.3. The catalyst sample (ca. 0.2 to 0.5 g) was placed in the sample cell, which was then heated up to 150^{o}C and held at this temperature for 3 h under reduced pressure of 10^{-3} mmHg. After the catalyst sample was cooled down to room temperature, nitrogen uptakes were measure as follows.

Step (1) Adsorption step: The sample that set in the sample cell was dipped into liquid nitrogen. Nitrogen gas that flowed through the system was adsorbed on the surface of the sample until equilibrium was reached.

Step (2) Desorption step: The sample cell with nitrogen gas-adsorption catalyst sample dipped into the water at room temperature. The adsorbed nitrogen gas was desorbed from the surface of the sample. This step was completed when the indicator line was in the position of base line.

Step (3) Calibration step: 1 ml of nitrogen gas at atmospheric pressure was injected through the calibration port of the gas chromatograph and the area was measured. The area was the calibration peak.

4.2.3 Scanning electron microscopy (SEM)

SEM was used to determine the catalyst morphologies. The SEM of JEOL mode JSM-5410LV was applied using the secondary electron mode at 15 kV.

4.2.4 Energy dispersive X-ray spectroscopy (EDX)

EDX was used to determine the elemental distribution and the quantitative elemental analysis throughout the catalyst granules. The EDX was performed using Link Isis series 300 program.

4.2.5 Temperature programmed reduction (TPR)

TPR was used to determine the reduction behaviors and reducibilities of the samples using a Micrometritics Chemisorb 2750.

1. The catalyst sample of 50 mg was used in the sample cell.
2. Prior to operation, the catalyst was heated up to 200^{o}C in flowing nitrogen and held at this temperature for 1 h.
3. After the catalyst sample was cooled down to room temperature, the carrier gas was 5% H_2 in Ar (30 cc/min) were ramping from 35 to 800 ^{o}C at 5^{o}C/min.
4. A cold trap was placed before the detector to remove water produced during the reaction.
5. A thermal conductivity detector (TCD) was used to determine the amount of hydrogen consumption during TPR.
6. The hydrogen consumption was calibrated using TPR of Ag_2O at the same conditions.

4.2.6 CO Chemisorptions

Static CO chemisorptions at room temperature on the reduce catalysts was used to determined the number of reduce surface cobalt metal atoms and overall cobalt dispersion. The total CO chemisorptions were calculated from the number of injection of a known volume. It was determined using a Micrometrics Pulse Chemisorb 2750 instrument. Prior to the chemisorptions, the catalyst sample about 0.20 g was reduced at 350^0C for 3 hours at ramping rate of 10^0C/min. After temperature decreased to the room temperature, carbon monoxide as known volume (86 microliter) was injected to catalyst and repeated until desorption peak constant. Amount of carbon monoxide adsorption on catalyst would relate to the amounts of active site.

4.3 Reaction study in CO_2 hydrogenation

CO_2 hydrogenation was used to determine the overall activity of catalyst samples. It was performed by using 0.1 g of catalyst samples packed in a middle of fixed-bed micro reactor, which was located in the electrical furnace. The total flow rate was 30 ml/min with the H_2/CO_2 ratio of 10/1. The catalyst sample was re-reduced in situ in flowing H_2 at 350^oC for 3 h prior to CO_2 hydrogenation. CO_2 hydrogenation was carried out at 220^oC and 1 atm. The effluent was analyzed using gas chromatography technique Thermal conductivity detector (TCD), molecular sieve 5 A^o was used for separation of carbon dioxide (CO_2) and carbon oxide (CO). Flame ionization detector (FID), VZ-10 was used for separation of light hydrocarbon such as methane (CH_4), ethane (C_2H_6), propane (C_3H_8), etc.

4.3.1 Apparatus

Flow diagram of CO_2 hydrogenation system is shown in Figure 4.1. The system consists of a reactor, an automatic temperature controller, an electrical furnace and a gas controlling system.

4.3.1.1 Reactor

The reactor was made from a stainless steel tube (O.D. 3/8”). Two sampling points were provided above and below the catalyst bed. Catalyst was placed between two quartz wool layers.

4.3.1.2 Automation Temperature Controller

This unit consisted of a magnetic switch connected to a variable voltage transformer and a solid-state relay temperature controller model no. SS2425DZ connected to a thermocouple. Reactor temperature was measured at the bottom of the catalyst bed in the reactor. The temperature control set point is adjustable within the range of 0-800^{o}C at the maximum voltage output of 220 volt.

4.3.1.3 Electrical Furnace

The furnace supplied heat to the reactor for CO_2 hydrogenation. The reactor could be operated from temperature up to 800^{o}C at the maximum voltage of 220 volt.

4.3.1.4 Gas Controlling System

Reactant for the system was each equipped with a pressure regulator and an on-off valve and the gas flow rates were adjusted by using metering valves.

4.3.1.5 Gas Chromatography

The composition of hydrocarbons in the product stream was analyzed by a Shimadzu GC14B (VZ10) gas chromatograph equipped with a flame ionization detector. A Shimadzu GC8A (molecular sieve 5A^{0}) gas chromatography equipped with a thermal conductivity detector was used to

analyze CO_2, CO and H_2 in the feed and product streams. The operating conditions for each instrument are shown in the Table 4.2.

Table 4.2 Operating condition for gas chromatograph.

Gas Chromagraph	SHIMADZU GC-8A	SHIMADZU GC-14B
Detector	TCD	FID
Column	Molecular sieve 5A	VZ10
- Column material	SUS	-
- Length	2 m	-
- Outer diameter	4 mm	-
- Inner diameter	3 mm	-
- Mesh range	60/80	60/80
- Maximum temperature	350^{o}C	80^{o}C
Carrier gas	He (99.999%)	H_2 (99.999%)
Carrier gas flow	40 cc/min	-
Column gas	He (99.999%)	Air, H_2
Column gas flow	40 cc/min	-
Column temperature		
- initial (^{o}C)	60	70
- final (^{o}C)	60	70
Injector temperature (^{o}C)	100	100
Detector temperature (^{o}C)	100	150
Current (mA)	80	-
Analysed gas	Ar, CO, H_2	Hydrocarbon C_1-C_4

4.3.2 Procedures

1. Using 0.1 g of catalyst packed in the middle of the stainless steel micro reactor, which is located in the electrical furnace.
2. The total flow rate was 30 ml/min with the H_2/CO_2 ratio of 10/1 in a fixed-bed flow reactor. A relatively high H_2/CO_2 ratio was used to minimize deactivation due to carbon deposition during reaction.
3. The catalyst sample was re-reduce *in situ* in flowing H_2 at 350 ^oC for 3 h prior to CO_2 hydrogenation.
4. CO_2 hydrogenation was carried out at 220 ^oC and 1 atm total pressure in flowing 9% CO in H_2.
5. The effluent was analyzed using gas chromatography technique. [Thermal conductivity detector (TDC) was used for separation of carbon monoxide (CO) and carbon dioxide (CO_2) and flame ionization detector (FID) were used for separation of light hydrocarbon such as methane (CH_4), ethane (C_2H_6), propane (C_3H_8), etc.] In all cases, steady-state was reached within 6 h. first analysis, after the CO_2 are fed into micro reactor at 5 minutes and analyzed every hour until 6 h.

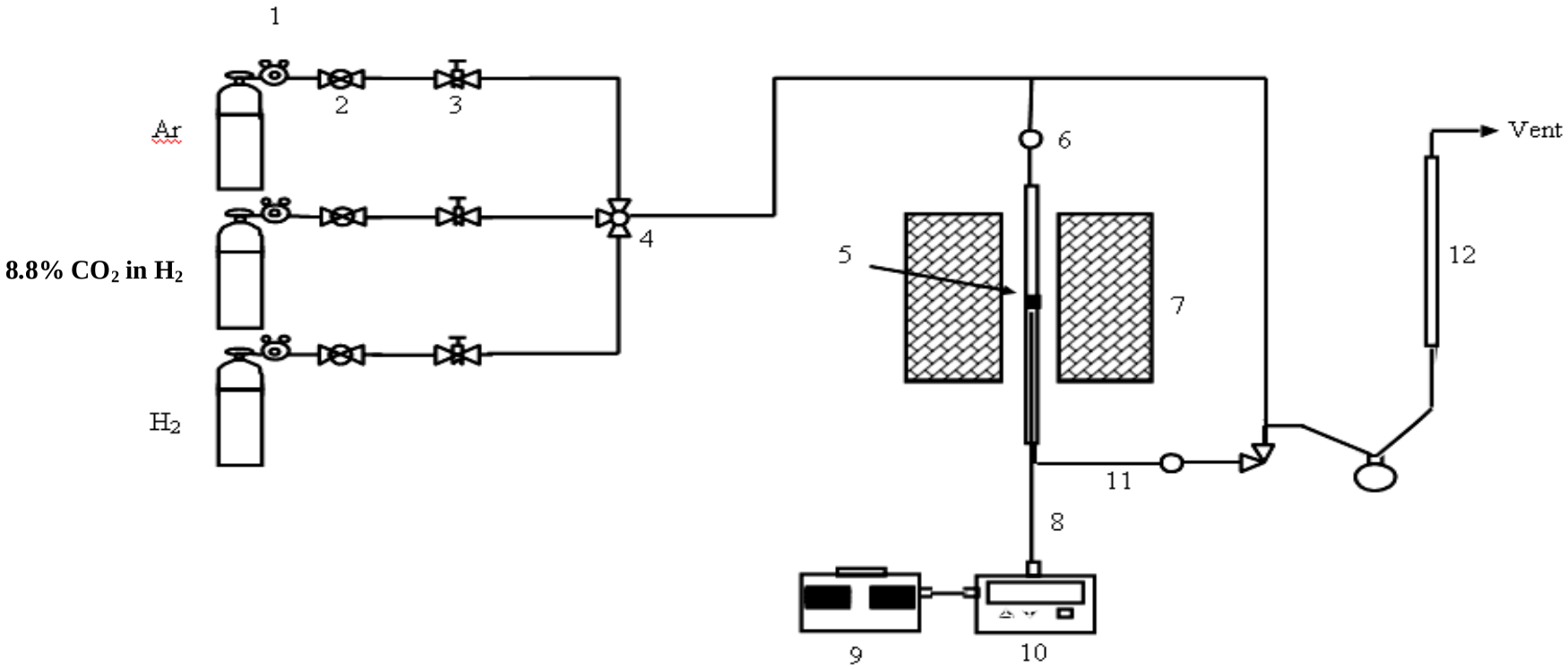

1. Pressure Regulator
2. On-Off Value
3. Metering Valve
4. 3-way Valve
5. Catalyst Bed
6 Sampling point
7.Furnace
8. Thermocouple
9. Variable Voltage Transformer
10. Temperature Controller
11. Heating Line
12. Bubble Flow Meter

Figure 4.1 Flow diagram of **CO_2 hydrogenation system**

4.4 Research Methodology

4.4.1 Part 1: Study of Co/ZrO_2 catalysts

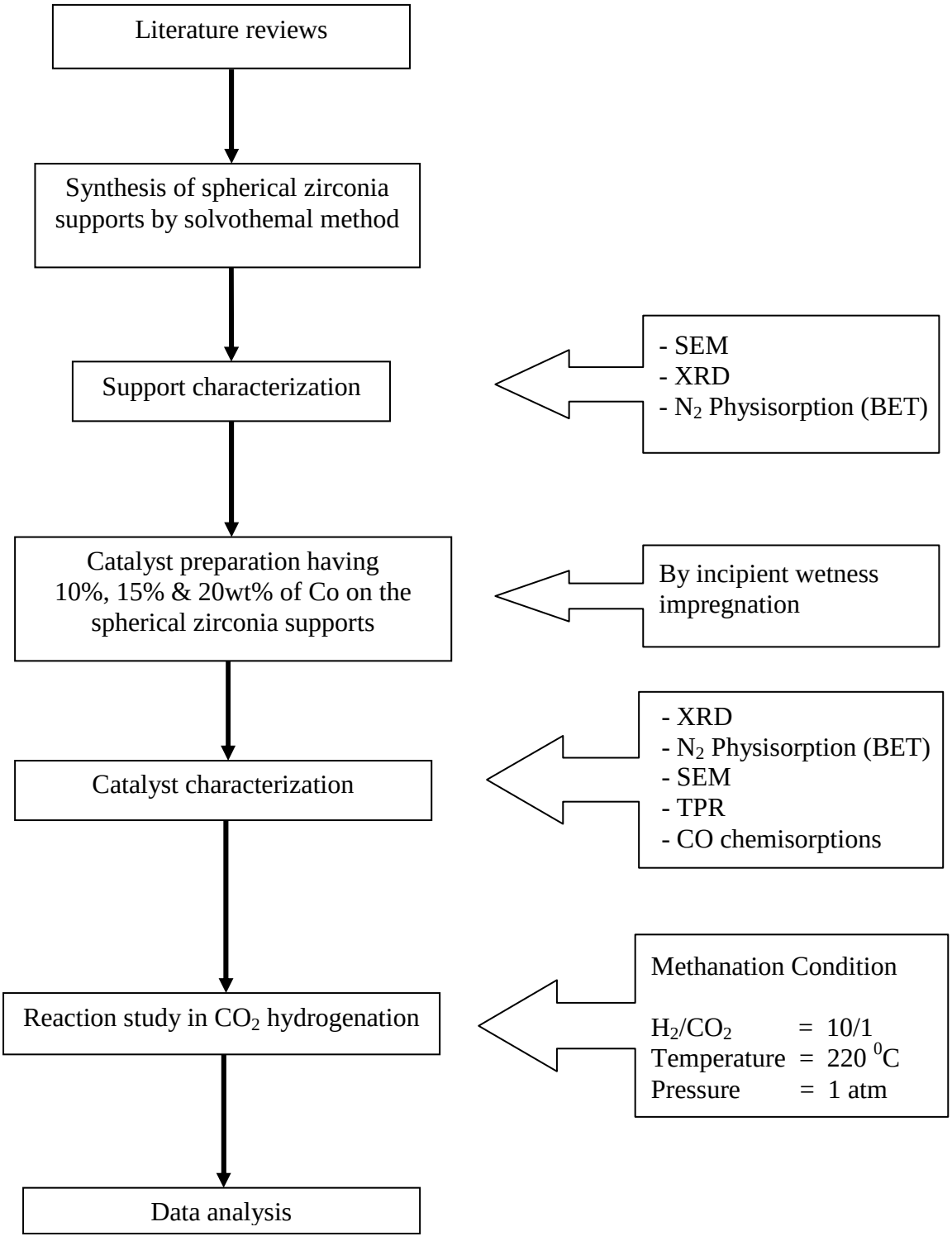

4.4.2 Part 2: Study of modified Ce-ZrO_2-supported Co catalysts, by sequential-impregnation method

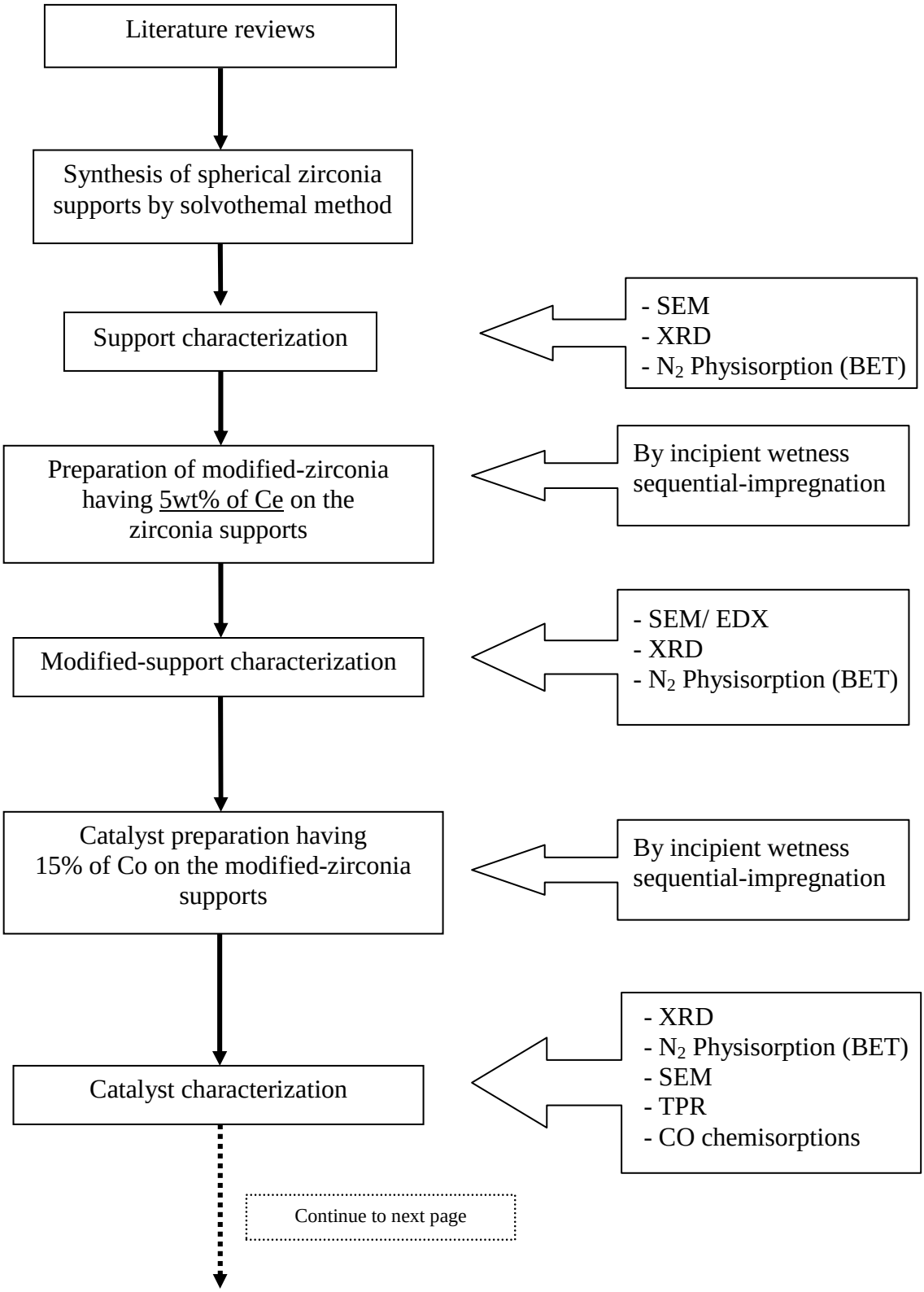

4.4.2 Part 2: Study of modified Ce-ZrO_2-supported Co catalysts, by sequential-impregnation method (Continuous)

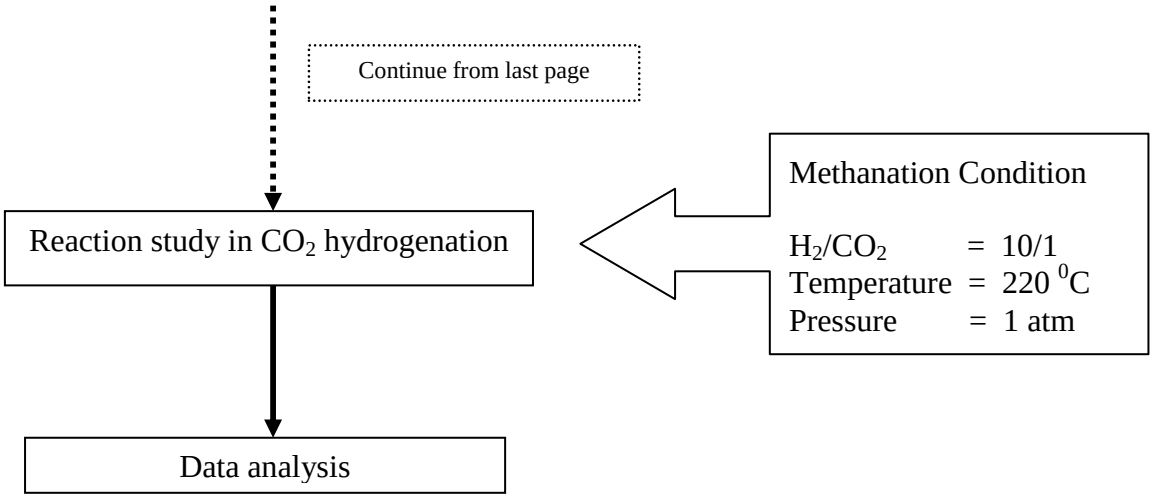

4.4.3 Part 3: Study of modified Ce-Co/ZrO_2 catalysts

by co-impregnation with cobalt method

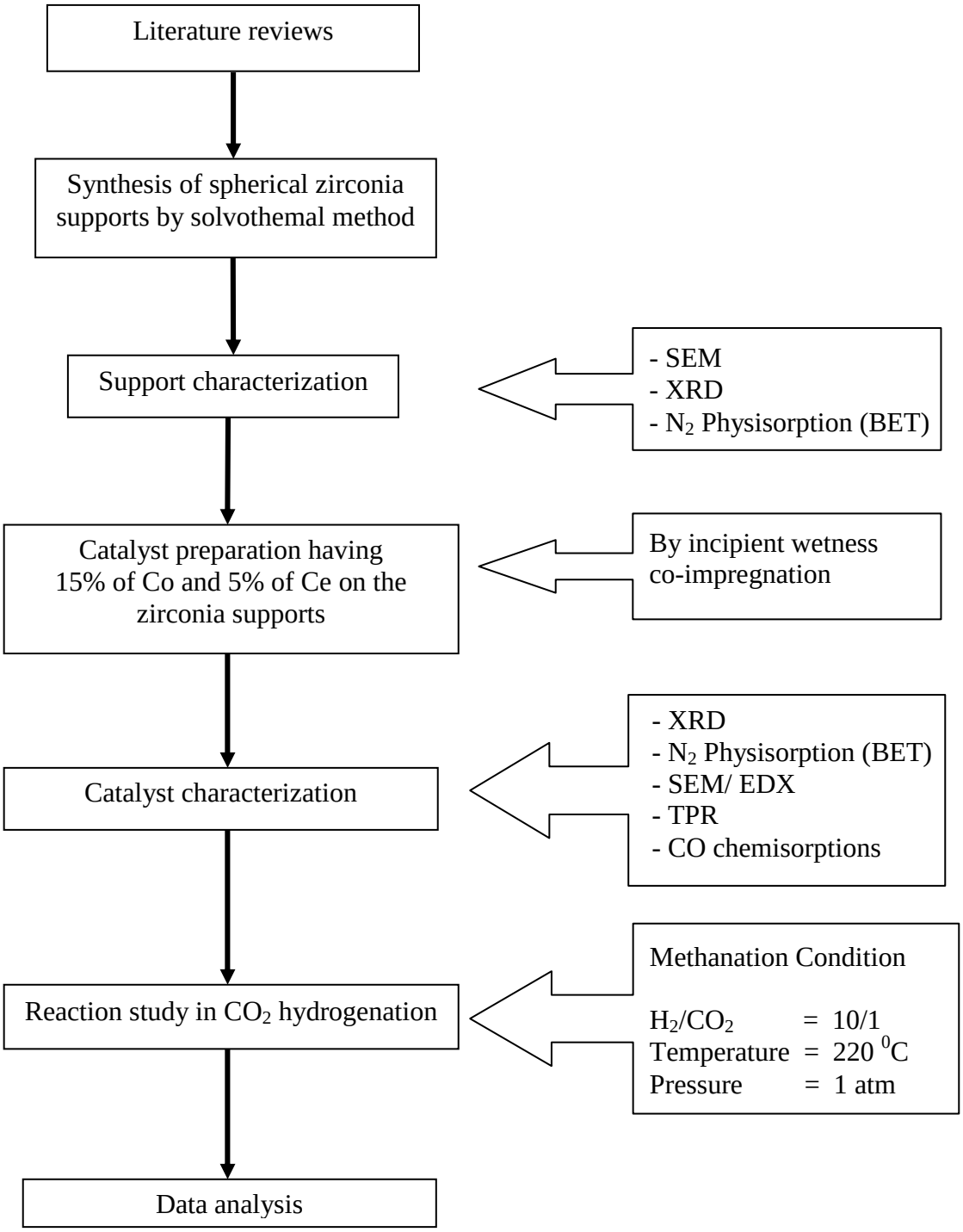

4.5 Catalysts nomenclature

The nomenclature was used for the catalyst samples in this study are as follows:

- BC ZrO_2
- AC ZrO_2
- 10Co/ZrO_2
- 15Co/ZrO_2
- 20Co/ZrO_2
- 5Ce/ZrO_2
- Co/Ce-ZrO_2
- Co-Ce/ZrO_2

BC ZrO_2 refers to spherical zirconia supports at before calcination.

AC ZrO_2 refers to spherical zirconia supports at after calcination.

10Co/ZrO_2 refers to spherical zirconia-supported cobalt catalyst at 10 wt% of cobalt loading.

15Co/ZrO_2 refers to spherical zirconia-supported cobalt catalyst at 15 wt% of cobalt loading.

20Co/ZrO_2 refers to spherical zirconia-supported cobalt catalyst at 20 wt% of cobalt loading.

5Ce/ZrO_2 refers to spherical zirconia-supported cerium catalyst at 5 wt% of cerium loading.

Co/Ce-ZrO_2 refers to modified-spherical zirconia-supported cobalt catalyst by adding cerium metal. Preparation method was the sequential- impregnation (15 wt% cobalt was loaded after 5 wt% cerium was modified)

Co-Ce/ZrO_2 refers to modified-spherical zirconia-supported cobalt catalyst by adding cerium metal. Preparation method was the co- impregnation (5 wt% cerium and 15 wt% cobalt were loaded together)

CHAPTER V

RESULTS AND DISCUSSION

This thesis investigated the characteristic and catalytic properties of spherical zirconia supported cobalt catalysts and modified-spherical zirconia support cobalt catalyst by adding a promoter is Cerium (Ce) on the spherical zirconia support for carbon dioxide hydrogenation reaction under methanation condition. In this chapter, the experimental results and discussions are described by divided into two sections. The first section described characteristics and catalytic properties of spherical zirconia supported cobalt catalysts (Co/ZrO_2). It was studied in terms of different cobalt loading, i.e., 10 wt%, 15 wt% and 20 wt%. The second section described characteristics and catalytic properties of modified-spherical zirconia support cobalt catalyst. It was studied in terms of different preparation, i.e., sequential-impregnation (cobalt was loaded after cerium was modified, $Co/Ce\text{-}ZrO_2$) and co-impregnation (cerium and cobalt were loaded together, $Co\text{-}Ce/ZrO_2$). The catalytic properties of both sections were studied in terms of CO_2 hydrogenation reaction under methanation condition.

5.1 Characteristics of the spherical zirconia supported cobalt catalysts (Co/ZrO_2)

5.1.1 X-ray diffraction (XRD)

X-ray diffraction is used to reveal the bulk crystalline phases and crystalline size of various catalyst samples because of its qualitative and nondestructive analysis. The crystalline phase identification was carried out on the basis of data from X-ray diffraction. The XRD patterns of spherical zirconia supports before and after calcinations (fresh ZrO_2 and calcined ZrO_2) and after cobalt loading (Co/ZrO_2), are shown in Fig. 5.1. After calcination in air at 450 ^oC for 3 h, all catalysts were tested by XRD. It was found that the zirconia supports exhibited the XRD patterns of both tetragonal and monoclinic zirconia, the slight diffraction peak of monoclinic can be observed at 24^0, 34^0, 42^0, 46^0 and 56^0. The diffraction peak of tetragonal can be observed at 30^0, 35^0, 51^0 and 60^0. However, with various cobalt

loadings, the samples also exhibited the XRD patterns of both tetragonal and monoclinic zirconia, but the peak intensity was much lower. It should be noted that the spherical zirconia-supported cobalt catalysts are stable upon the tetragonal phase zirconia. The Co_3O_4 peaks for the cobalt catalysts can be seen at 37^0 and 65^0 especially for $20Co/ZrO_2$.

Typically, the monoclinic phase is stable to ≈ 1170 ^{0}C, at which temperature it transforms into the tetragonal phase, which is stable up to 2370 ^{0}C [P.D.L. Mercera *et al*., 1991]. At low temperature, a metastable tetragonal phase zirconia is usually observed when zirconia is prepared by certain methods such as precipitation from aqueous salt solution or thermal composition of zirconium salts as employed in this work [J. Panpranot *et al*., 2006]. The transformation of the metastable tetragonal into the monoclinic was probably due to the lower surface energy of the tetragonal phase compared to monoclinic phase [E. Tani *et al*., 1983; M.I. Osendi *et al*., 1985].

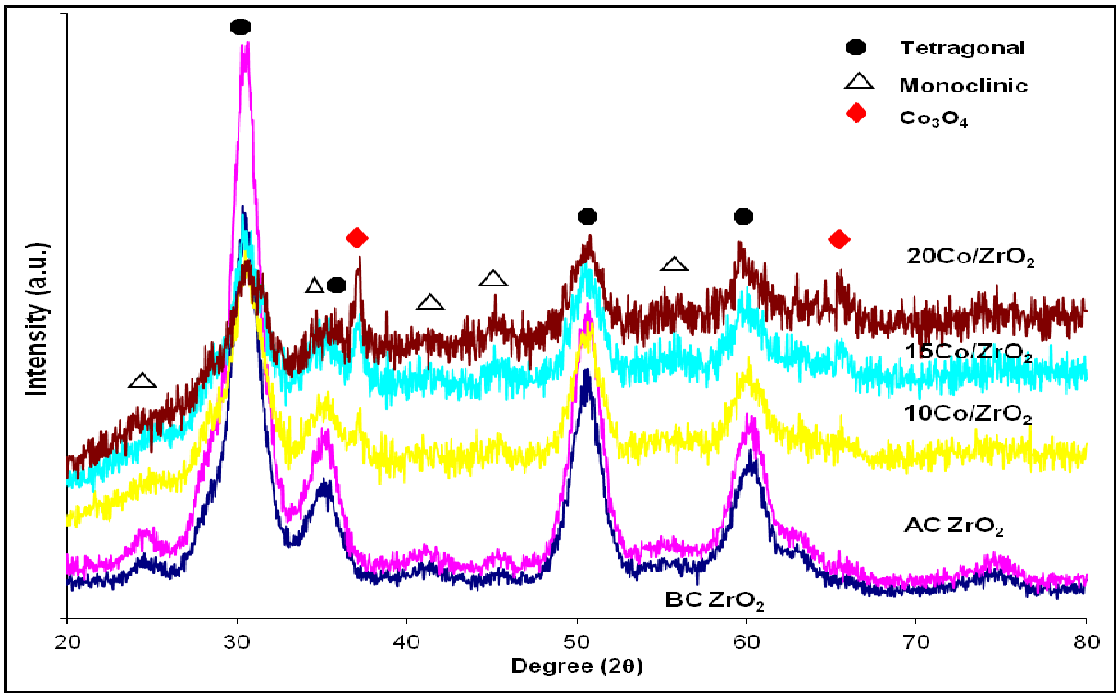

Figure 5.1 XRD patterns of various zirconia supports and various cobalt loadings of spherical zirconia-supported cobalt catalysts

5.1.2 Scanning electron microscopy (SEM)

The scanning electron micrographs (SEM) of zirconia supports before calcinations, before and after cobalt loading are shown in Fig.1. It was found that the zirconia prepared by 1,4–butanediol as a solvent under solvolthermal reaction of zirconium tetra-n-butoxide exhibited a spherical shape with an average particle size of 4.0-4.7 μm for before calcination [in Fig.1. (a) and (b)]. An average particle size of 3.2-3.8 μm after calcinations prior to cobalt loading [in Fig.1. (c)] was observed. An average particle size of 3.9-4.7 μm after calcinations and loaded with various wt% cobalt were evident. Fig.5.2. (d), (e) and (f) show that the cobalt loaded was apparently located on the outer surface of zirconia. The morphology of zirconia was also stable even after cobalt loading.

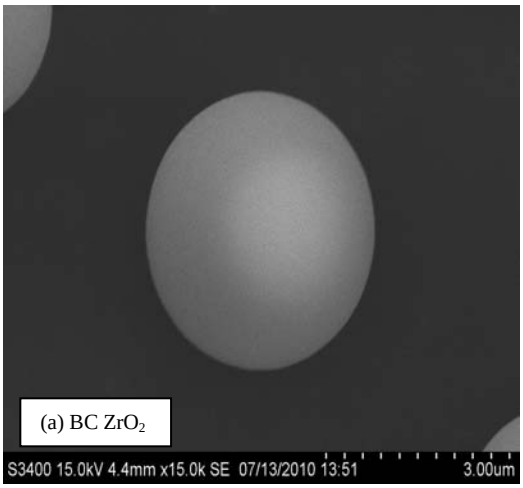

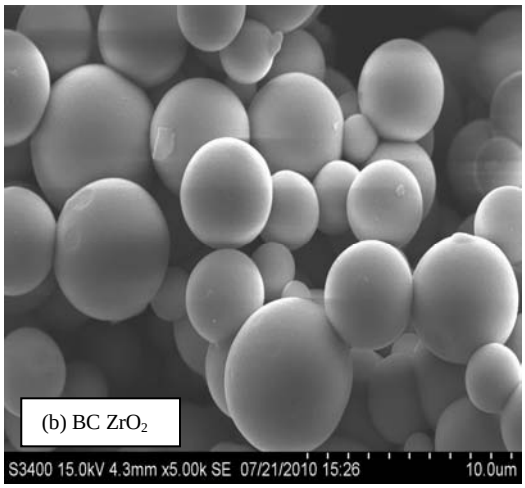

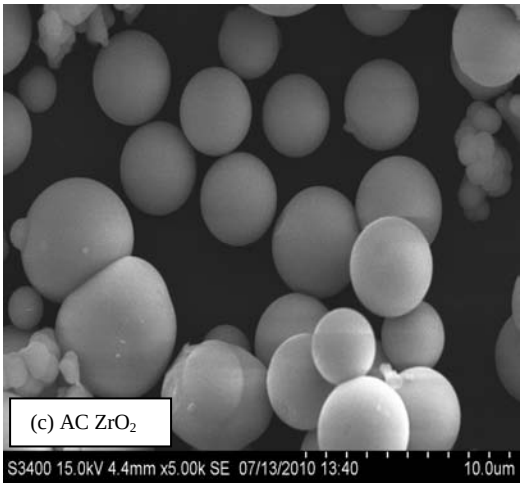

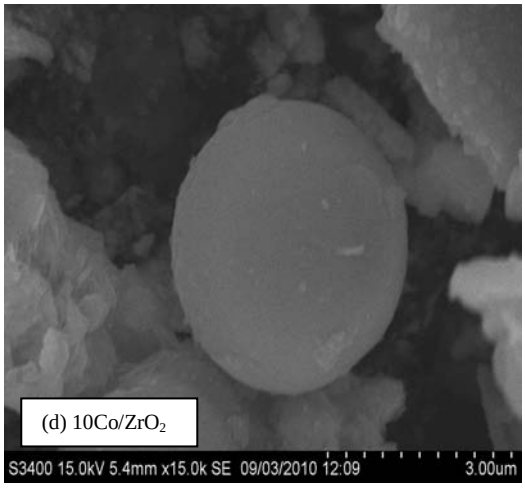

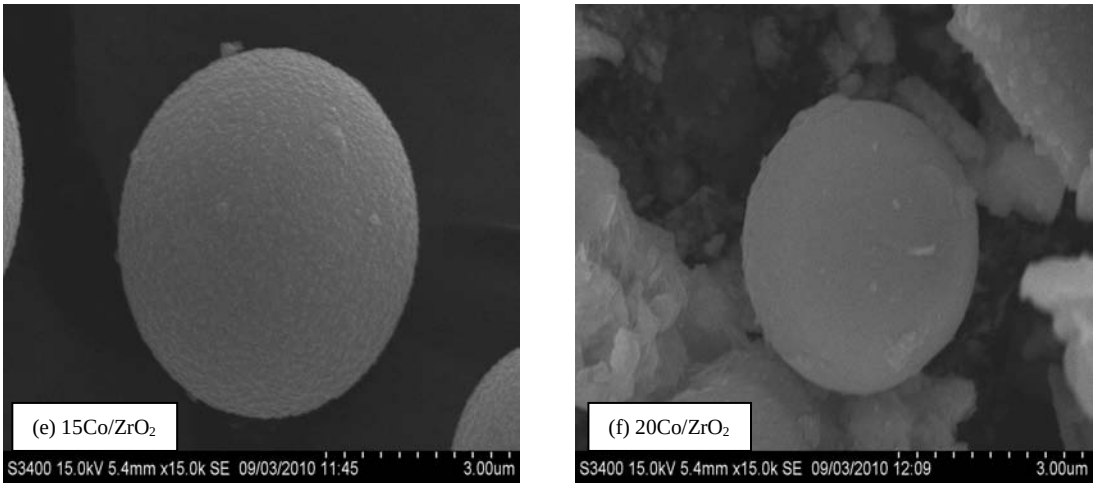

Fig. 5.2 SEM micrographs of (a) and (b) zirconia support before calcinations,

(c) zirconia support after calcinations before cobalt loading,

(d) 10 wt% cobalt loading on zirconia, (e) 15 wt% cobalt loading on zirconia

(f) 20 wt% cobalt loading on zirconia

5.1.3 Temperature-programmed reduction (TPR)

Temperature-programmed reduction (TPR) was used to determine the reduction behaviors and reducibilities of samples. The TPR profiles of cobalt loading on spherical zirconia-supported cobalt catalysts are shown in Fig. 5.3 and Table 5.1. It was found the reduction temperature and % reducibilities of the calcined catalysts of cobalt loading at 10 wt%, 15 wt% and 20 wt% exhibited similar patterns. This indicated that the strong interaction between cobalt and zirconia support of 20 wt%, 15 wt% and 10 wt% of cobalt loading were similar exhibition. The reduction temperature was slightly shifted to higher temperatures with the increasing amount of cobalt loading in zirconia support. The different peak indicated to different cobalt oxide (Co_xO_y) species which was reduced to be more stable form. This first peak has been ascribed the reduction of Co_3O_4 to CoO, followed by the second peak which corresponds to the reduction of CoO to Co [Borg, Ø. *et al*., 2007].

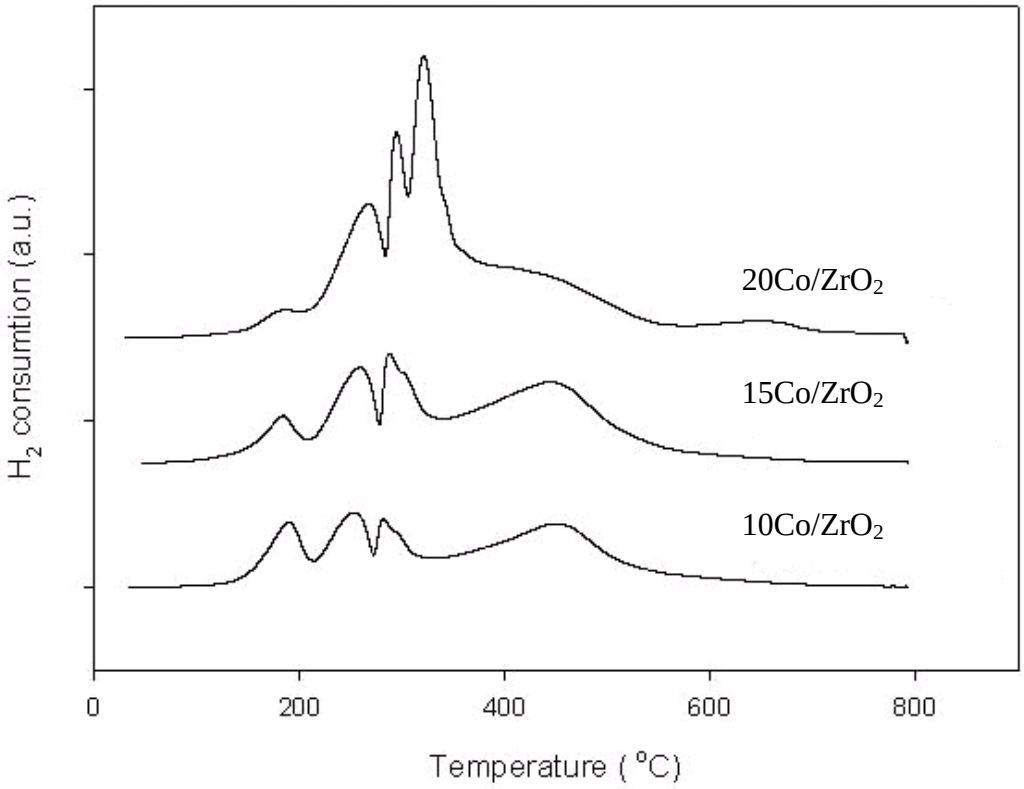

Fig. 5.3 TPR profiles of various wt% of cobalt loadings on spherical zirconia-supports

5.1.4 N_2 physisorption (BET)

N_2 physisorption (BET) measurement was used to determine the amount of surface area, cumulative volume of pore and average pore diameter of the samples. It is listed in Table 5.1. The surface area and cumulative volume of pore were found in the order of 10 wt% > 15 wt% > 20 wt% of cobalt loading, respectively. In addition, it also shows that the spherical zirconia supported has surface area and pore volume that could support the loading of the appropriate 20wt% of cobalt from this study.

Table 5.1 The characteristics of Co/ZrO_2 catalyst

Sample	%Reducibility	BET surface area (m^2/g)	Pore volume (cm^3/g)	Pore diameter (nm)
AC ZrO_2	-	159	0.170	2.843
$10Co/ZrO_2$	54.2	139	0.145	2.831
$15Co/ZrO_2$	51.8	116	0.129	2.838
$20Co/ZrO_2$	49.3	115	0.123	3.012

5.1.5 CO Chemisorptions

The CO chemisorption was used to determine the number of reduce surface or active site cobalt metal atoms and overall cobalt dispersion. The CO chemisorption results of various cobalt catalyst are shown in Table 5.2. It was found that the number of reduce surface or active site cobalt metal atoms and %dispersion of 20 wt% ≈ 15 wt% > 10 wt% of cobalt loading, respectively. It was indicated that active size and dispersion of cobalt metal at 20 wt% similar to 15 wt%.

Table 5.2 The characteristics of Co/ZrO_2 catalyst in term of CO chemisorptions.

Sample	Active site molecule (x 10^{19} mol g cat.-1)	% Co dispersion[a]
$10Co/ZrO_2$	1.19	1.18
$15Co/ZrO_2$	1.80	0.90
$20Co/ZrO_2$	1.83	1.16

[a] Based on Co adsorption

$$\% \text{ Dispersion} = \frac{Amount\ of\ reduced\ Co\ metal}{Amount\ of\ loaded\ Co} \times 100$$

5.2 Reaction study in CO_2 hydrogenation

CO_2 hydrogenation was the reaction in this study. CO_2 is converted to light hydrocarbon such as methane (CH_4), ethane (C_2H_6), propane (C_3H_8), etc. The CO_2 hydrogenation was used to determine the overall activity in order to measure the catalytic properties of catalyst sample with a various wt% of cobalt loadings. The results are shown in Table 5.3. It indicated that the reaction rate increased in the order of 20 wt% > 15 wt% > 10 wt% of cobalt loading. Considering $\%CO_2$ conversion, it also increased in the order of 20 wt% > 15 wt% > 10 wt% of cobalt loading. For selectivity to methane, it was found that it was similar for all catalyst samples. No changes in methane selectivity were found.

Table 5.3 Catalytic activities of Co/ZrO_2 catalyst in CO_2 hydrogenation under methanation condition

Sample	Reaction rate ($x10^2$ g CH_2/ g cat· h)	CO_2 conversion % conversion	Product selectivity (%) CH_4	CO
$10Co/ZrO_2$	16.3	25.4	97.0	3.0
$15Co/ZrO_2$	29.7	45.1	98.7	1.3
$20Co/ZrO_2$	33.5	50.9	98.9	1.1

5.3 Characteristics of modified-spherical zirconia-supported cobalt catalyst

By addition cerium (Ce) to the spherical zirconia-supported cobalt catalyst ($Co/Ce\text{-}ZrO_2$) and ($Co\text{-}Ce/ZrO_2$)

The second section described characteristics and catalytic properties of spherical zirconia supported-cerium catalyst ($5Ce/ZrO_2$) and modified-spherical zirconia-supported cobalt catalyst. For the modified-spherical zirconia-supported cobalt catalyst, it was studied in terms of different preparation, i.e., sequential-impregnation (15 wt% cobalt was loaded after 5 wt% cerium was modified, $Co/Ce\text{-}ZrO_2$) and co-impregnation (5 wt% cerium and 15 wt% cobalt were loaded together, $Co\text{-}Ce/ZrO_2$).

5.3.1 X-ray diffraction (XRD)

The XRD patterns of spherical zirconia support (ZrO_2), spherical zirconia-supported cobalt catalyst ($15Co/ZrO_2$), spherical zirconia-supported cerium catalyst ($5Ce/ZrO_2$) and modified-spherical zirconia-supported cobalt catalyst, i.e., the sequential-impregnation ($Co/Ce\text{-}ZrO_2$) and the co-impregnation ($Co\text{-}Ce/ZrO_2$) are shown in Fig. 5.2. The samples also exhibited the XRD patterns of both tetragonal and monoclinic zirconia, but the intensity of peak was decreased when cerium was added on zirconia support ($5Ce/ZrO_2$), and even more decreased when cerium and cobalt were added on zirconia ($Co/Ce\text{-}ZrO_2$ and $Co\text{-}Ce/ZrO_2$). This figure shows that the intensity was in the range of $15Co/ZrO_2$ > AC ZrO_2 > $5Ce/ZrO_2$ > $Co/Ce\text{-}ZrO_2$ > $Co\text{-}Ce/ZrO_2$. For both modified spherical zirconia- supported cobalt catalyst having low intensity, this indicated that zirconia support was completely covered by cerium and cobalt or perhaps the particle size of both modified spherical zirconia-supported cobalt catalyst were smaller than 5 nm which was invisible by XRD.

It was found that the zirconia supports exhibited the XRD patterns of both tetragonal and monoclinic zirconia, the slight diffraction peak of monoclinic can be observed at 24^0, 34^0, 42^0, 46^0 and 56^0. The diffraction peak of tetragonal can be observed at 30^0, 35^0, 51^0 and 60^0. However, all the samples also exhibited the XRD patterns of both tetragonal and monoclinic zirconia. In addition, the peak intensity was decreased when loading with Ce and more decreased when loading with Ce and

Co together. It should be noted that the spherical zirconia-supported cobalt catalysts are stable upon the tetragonal phase zirconia. The Co_3O_4 peaks for the cobalt catalysts can be seen at 37^0 and 65^0 especially for $15Co/ZrO_2$.

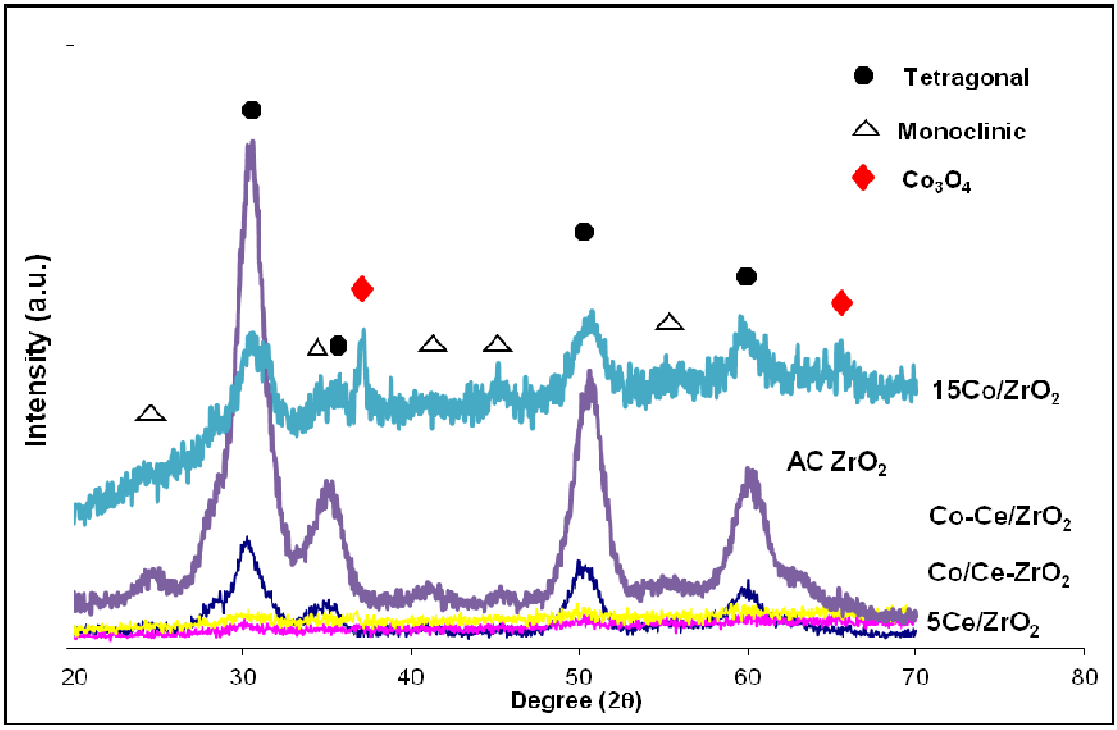

Figure 5.4 XRD patterns of various catalysts and support.

5.3.2 Scanning electron microscopy and energy dispersive X-ray spectroscopy (SEM/EDX)

The scanning electron micrographs (SEM) of spherical zirconia supported cerium catalyst ($5Ce/ZrO_2$) and modified-spherical zirconia-supported cobalt catalyst, i.e., the sequential-impregnation ($Co/Ce\text{-}ZrO_2$) and the co-impregnation ($Co\text{-}Ce/ZrO_2$) are shown in Fig.5.5. It was found that all samples still exhibited the spherical shape. $5CeZrO_2$ has particle size of 2.3-3.5 μm (average 2.9 μm), $Co/Ce\text{-}ZrO_2$ has particle size of 2.2-3.5 μm (average 3.1 μm) and $Co\text{-}Ce/ZrO_2$ has particle size of 2.0-3.1 μm (average 2.5 μm). Fig.5.5. (c) and (d) show the cobalt that was last loaded, it was apparently located on the outer surface of ceria-zirconia support. Fig.5.5. (e) and (f)

show the cobalt and cerium that was co loaded, it was apparently located on the outer surface of zirconia support.

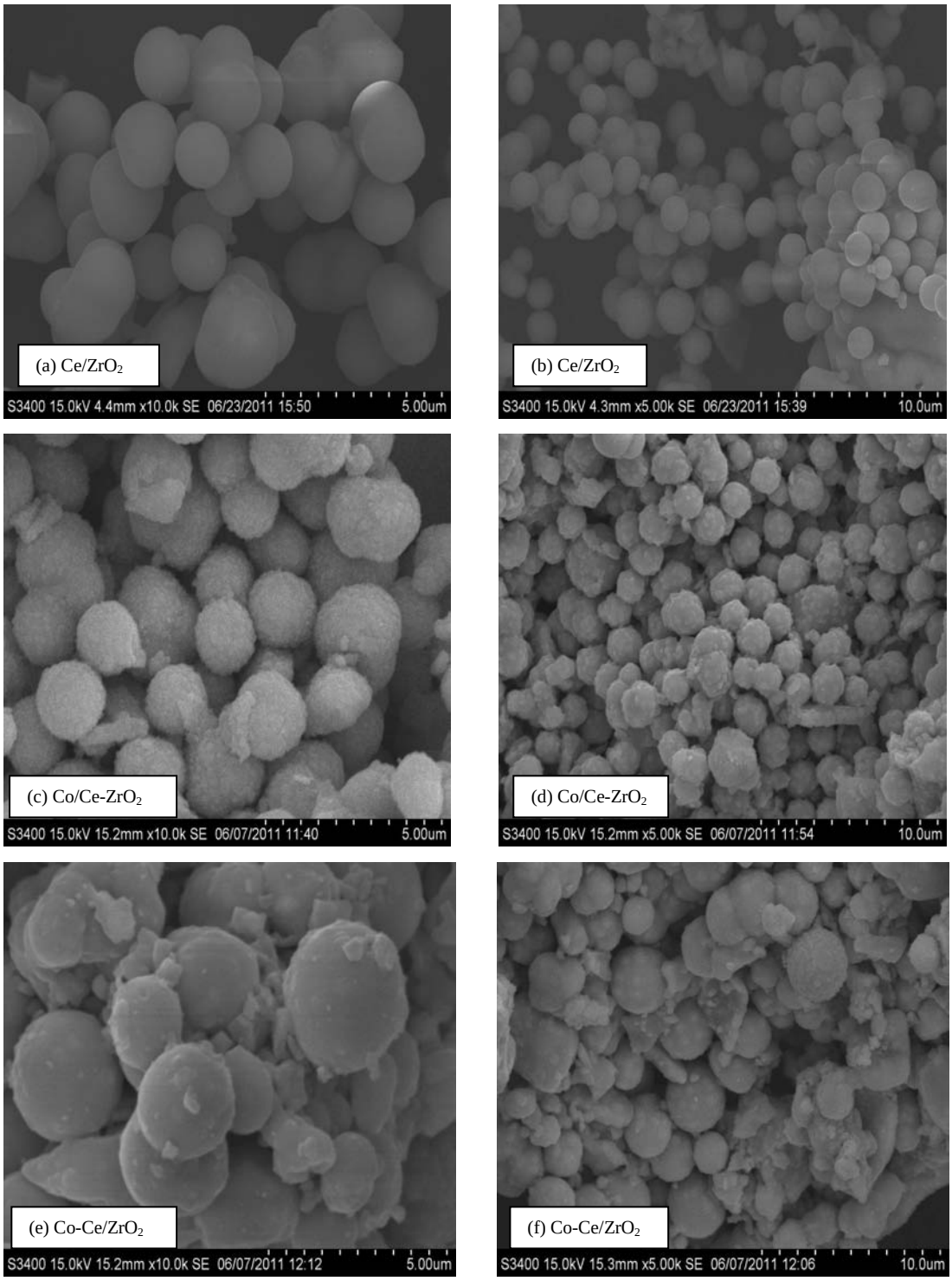

Fig. 5.5 SEM micrographs of different catalyst samples

The measurement curve for the quantitative elemental analysis throughout the catalyst granules of $5Ce/ZrO_2$, $Co/Ce\text{-}ZrO_2$ and $Co\text{-}Ce/ZrO_2$ using EDX measurement is shown in Figures 5.6, 5.7 and 5.8, respectively. The amounts of elements in the various catalysts are also listed below. It can be seen that the amounts of elements in various supports varied due to the adsorption ability of each support. Results show that the amount of element at the external surface of $5Ce/ZrO_2$, $Co/Ce\text{-}ZrO_2$ and $Co\text{-}Ce/ZrO_2$ was similar to that with loading.

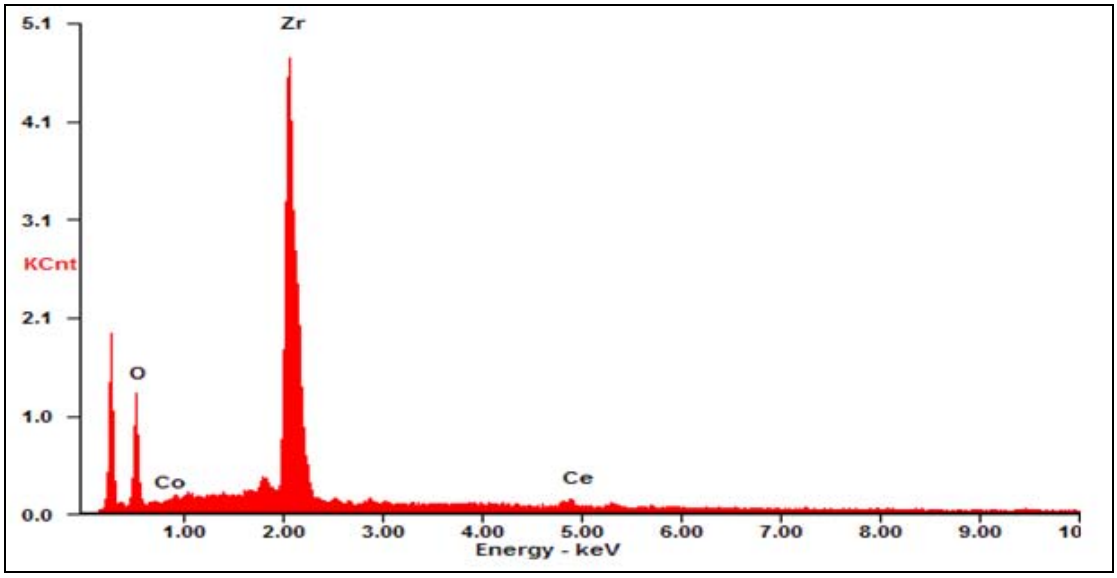

Element	Element(%)	Atomic(%)
O	20.10	59.70
Co	00.00	00.00
Zr	73.06	38.00
Ce	06.81	02.31

Figure 5.6 A spectrum of the $5Ce/ZrO_2$ catalyst from EDX analysis.

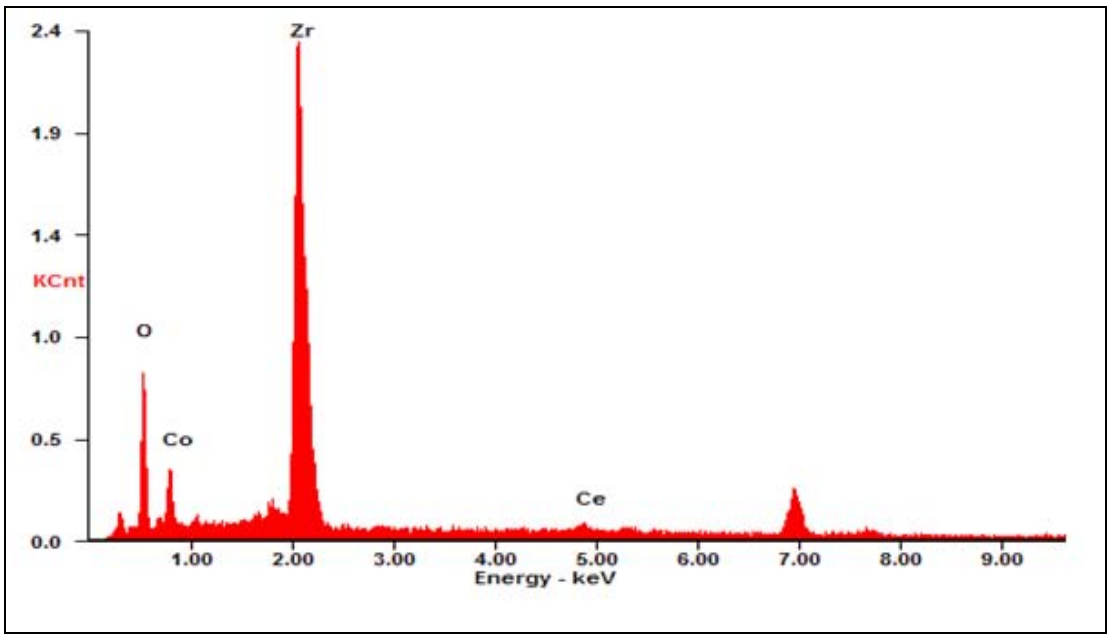

Element	Element(%)	Atomic(%)
O	16.21	50.68
Co	15.76	13.37
Zr	60.97	33.43
Ce	07.06	02.52

Figure 5.7 A pectrum of the Co/Ce-ZrO_2 catalyst from EDX analysis.

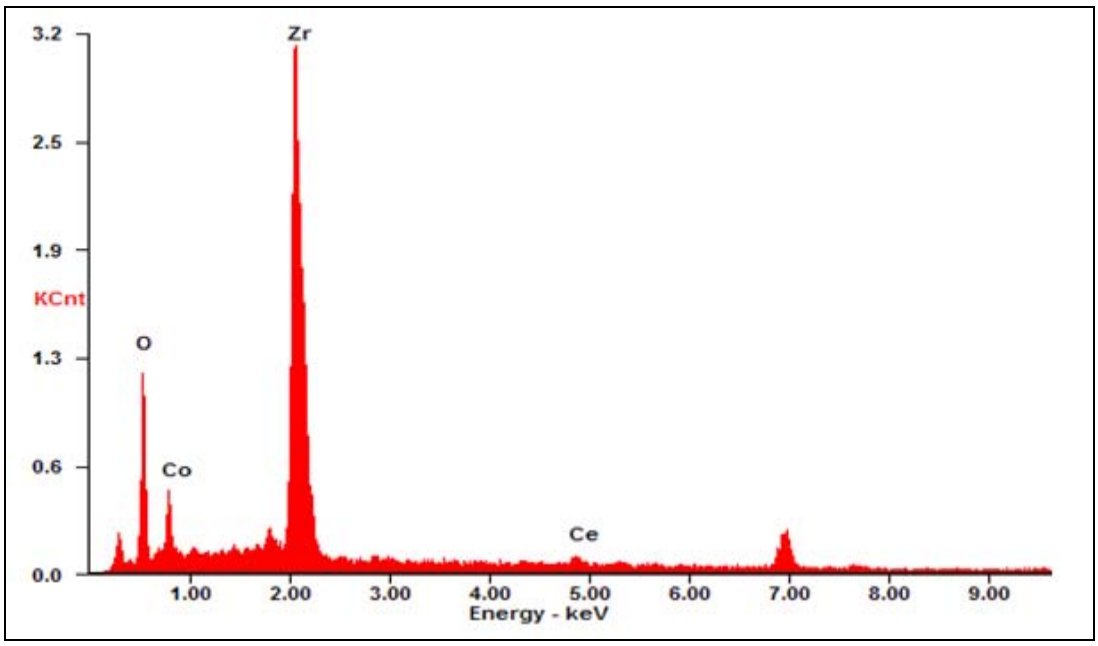

Element	Element(%)	Atomic(%)
O	18.35	54.08
Co	16.34	13.08
Zr	60.19	31.12
Ce	05.12	01.72

Figure 5.8 A spectrum of the Co-Ce/ZrO_2 catalyst from EDX analysis.

Besides the content of Co and Ce on the supports, one should consider the distribution of Co and Ce on the supports. SEM and EDX were also conducted in order to study the morphologies and elemental distribution of the samples, respectively. The typical SEM micrographs along with the EDX mapping for 5Ce/ZrO_2 (for Ce, Zr and O), Co/Ce-ZrO_2 (for Co, Ce, Zr and O) and Co-Ce/ZrO_2 (for Co, Ce, Zr and O) samples are illustrated in Figures 5.9, 5.10 and 5.11, respectively.

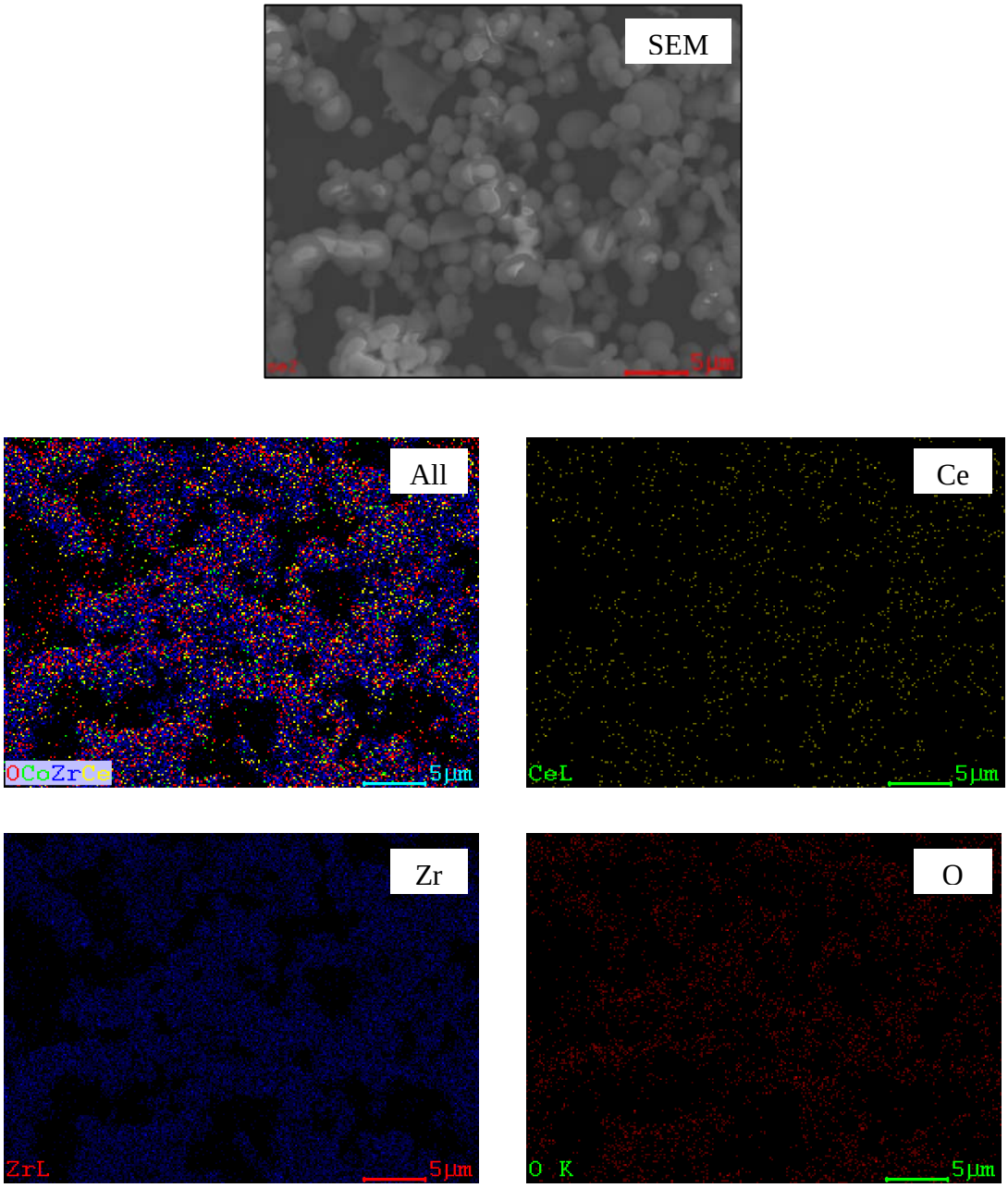

Figure 5.9 SEM micrograph and EDX mapping of the Ce/ZrO_2 catalysts.

For $5Ce/ZrO_2$ in figures 5.9, the spots on the catalyst granules represent concentrations of cerium oxides species at the external surface of the sample granule. It can be seen that the Ce oxide species show good distribution on the surface of zirconia support.

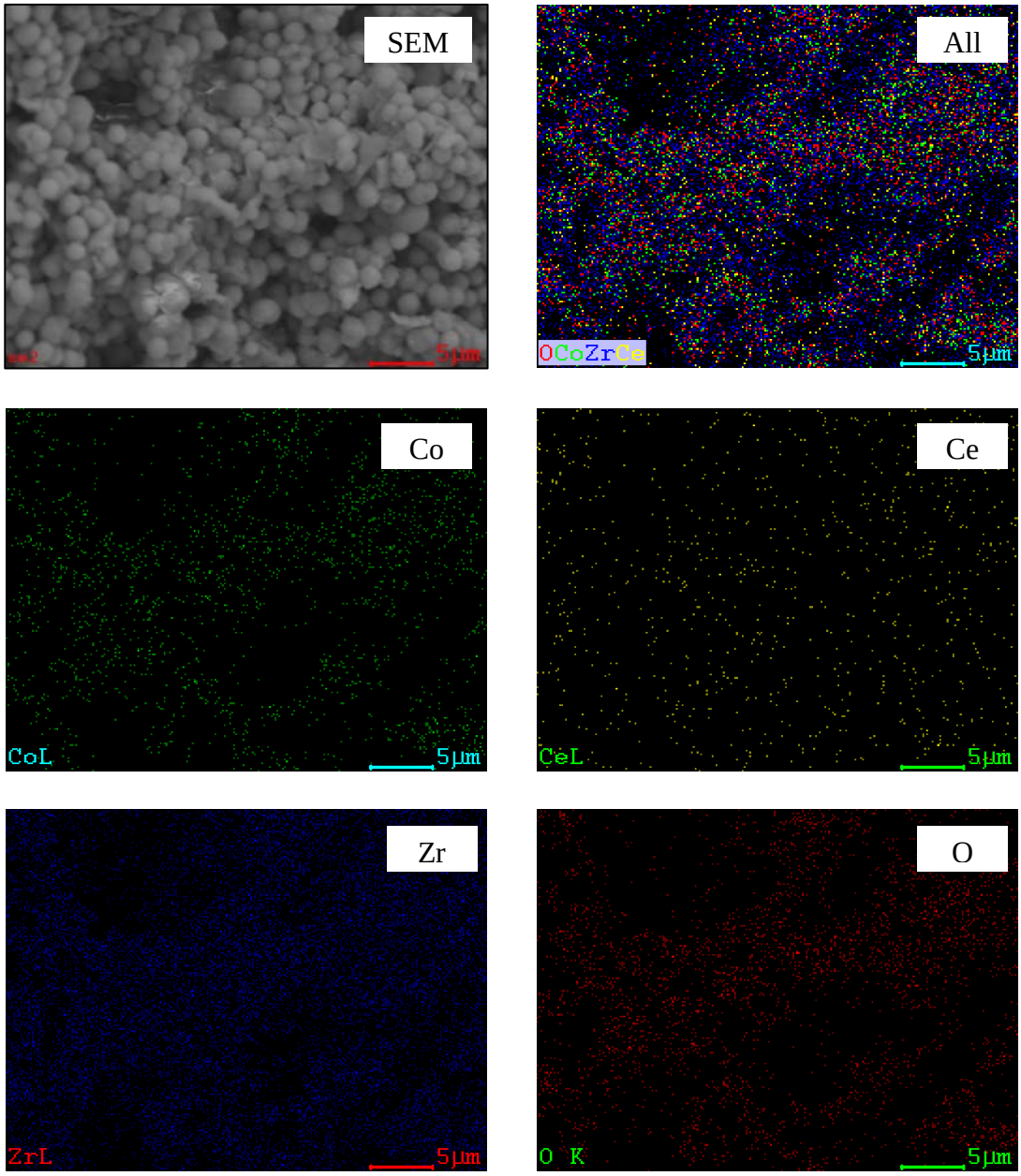

Figure 5.10 SEM micrograph and EDX mapping of the Co/Ce-ZrO_2 catalyst

For Co/Ce-ZrO_2 in figures 5.10, the spots on the catalyst granules represent concentrations of cobalt oxides and cerium oxides species, respectively at the external surface of the sample granule. It can be seen that the Co and Ce oxide species show good distribution on the surface of zirconia support.

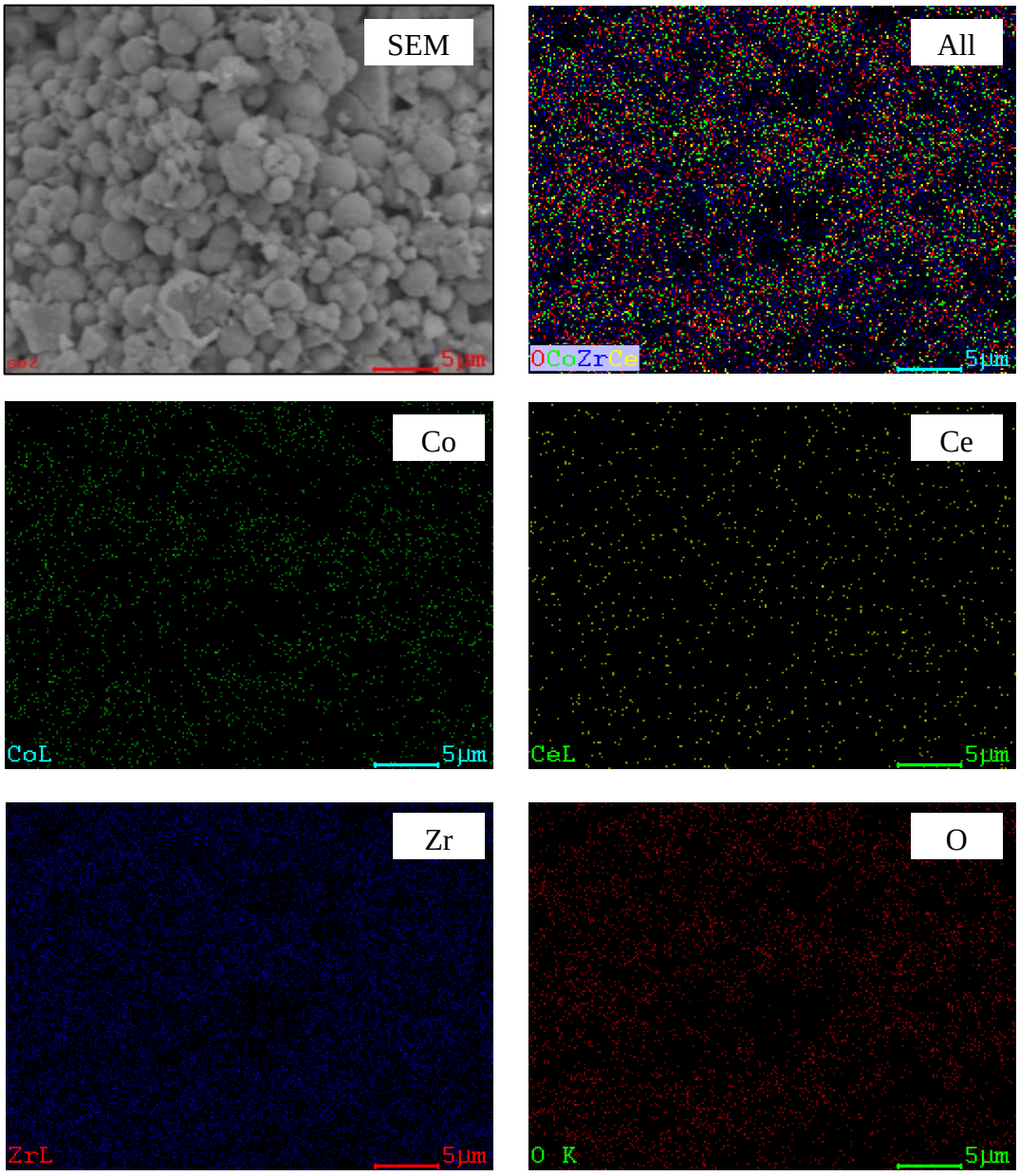

Figure 5.11 SEM micrograph and EDX mapping of the Co-Ce/ZrO_2 catalyst

For Co-Ce/ZrO_2 in figures 5.11, the green and yellow spots on the catalyst granules represent concentrations of cobalt oxides and cerium oxides species, respectively at the external surface of the sample granule. It can be seen that the Co and Ce oxide species show good distribution on the surface of zirconia support.

Results indicate that base on SEM micrographs and EDX mapping for all samples, they exhibited similar trends of morphologies and elemental distributions.

5.3.3 Temperature-programmed reduction (TPR)

Temperature-programmed reduction (TPR) was used to determine the reduction behaviors and reducibilities of the calcined catalyst. The TPR profiles of $5Ce/ZrO_2$, $15Co/ZrO_2$, $Co/Ce\text{-}ZrO_2$ and $Co\text{-}Ce/ZrO_2$ are shown in Fig. 5.12.

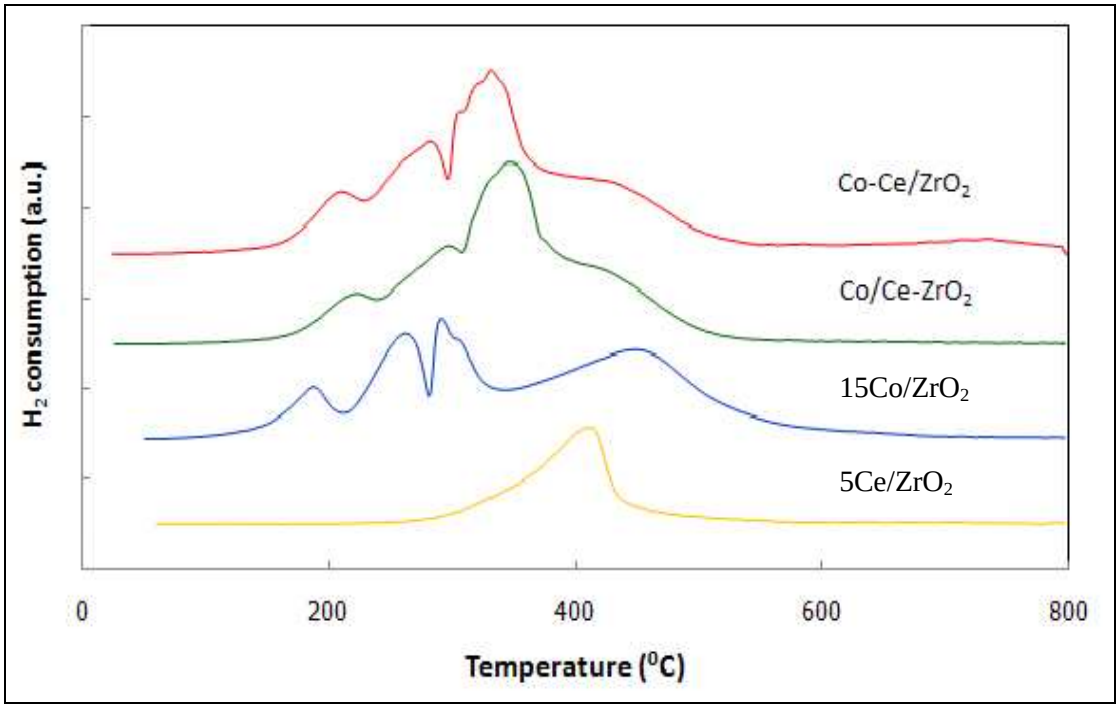

Fig. 5.12 TPR profiles of various catalyst samples.

By comparison of temperature at highest peak of each curve, it was found that the temperature of $5Ce/ZrO_2$ was 410 ^{0}C, $15Co/ZrO_2$ was 300 ^{0}C, $Co/Ce\text{-}ZrO_2$ was 350 ^{0}C, and $Co\text{-}Ce/ZrO_2$ was 330 ^{0}C.

By comparison of amount area under each curve, it was found that the area was in the order of $Co/Ce\text{-}ZrO_2$ > $Co\text{-}Ce/ZrO_2$ > $15Co/ZrO_2$ > $5Ce/ZrO_2$. It indicated that the reducibility was in the order of $Co/Ce\text{-}ZrO_2$ > $Co\text{-}Ce/ZrO_2$ > Co/ZrO_2 > Ce/ZrO_2.

From both comparison, it should be mentioned that interaction between Co and Ce occurred resulting in increase reducibilities of catalyst. On the other hand, Ce

can facilitate the reduction of cobalt catalyst. It was also found that the reduction temperature and trend of curve of the Co/Ce-ZrO_2 resembled with Co-Ce/ZrO_2 indicating that the strong interaction between cobalt, cerium and zirconia support of Co/Ce-ZrO_2 was similar to that of Co-Ce/ZrO_2 catalyst.

5.3.4 N_2 physisorption (BET)

N_2 physisorption (BET) measurement was used to determine the amount of surface area, cumulative volume of pore and average pore diameter of the samples. The physical properties of 5Ce/ZrO_2, 15Co/ZrO_2, Co/Ce-ZrO_2 and Co-Ce/ZrO_2 are shown in Table 5.4. It shows that the surface area and cumulative volume of pore of Co/Ce-ZrO_2 were similar to Co-Ce/ZrO_2 indicating that both catalysts has similar physical properties.

Table 5.4 The characteristics of various catalyst**s**

Sample	BET surface area (m^2/g)	Pore volume (cm^3/g)	Pore diameter (nm)
5Ce/ZrO_2	144	0.154	2.800
15Co/ZrO_2	116	0.129	2.838
Co/Ce-ZrO_2	102	0.107	2.794
Co-Ce/ZrO_2	104	0.112	2.787

5.3.5 CO Chemisorptions

The CO chemisorption was used to determine the number of reduce surface or active site cobalt metal atoms and overall cobalt dispersion. The CO chemisorption results of 5Ce/ZrO_2, 15Co/ZrO_2, Co/Ce-ZrO_2 and Co-Ce/ZrO_2 catalyst are shown in Table 5.5. It was found that the number of reduce surface or active site metal atoms were in the range of Co/Ce-ZrO_2 > 15Co/ZrO_2 > Co-Ce/ZrO_2 >

$5Ce/ZrO_2$. It showed that $5Ce/ZrO_2$ has low activity. The $Co/Ce\text{-}ZrO_2$ exhibited higher activity and metal dispersion than $15Co/ZrO_2$ and those of $Co\text{-}Ce/ZrO_2$ indicating that modified-spherical zirconia-supported cobalt catalyst by adding a promoter is Cerium (Ce). Using the sequential-impregnation. It should be mentioned that the addition of cerium oxide (CeO_2) to zirconium oxide (ZrO_2) results in improving the total active sites of catalyst and %dispersion of cobalt. But using the co-impregnation, cerium may be blocked to the active site of cobalt (when compared between $15Co/ZrO_2$ and $Co\text{-}Ce/ZrO_2$).

Table 5.5 The characteristics of various catalysts in term of CO chemisorptions.

Sample	Active site molecule (x 10^{19} mol g cat.$^{-1}$)	% Co dispersion[a]	% Ce dispersion[b]
$5Ce/ZrO_2$	0.23	-	1.06
$15Co/ZrO_2$	1.80	0.88	-
$Co/Ce\text{-}ZrO_2$	1.95	1.27	-
$Co\text{-}Ce/ZrO_2$	1.25	0.82	-

[a] Based on total amount of cobalt

[b] Based on total amount of cerium

5.4 Reaction study in CO_2 hydrogenation of modified-spherical zirconia support cobalt catalyst

CO_2 hydrogenation was the reaction in this study. CO_2 is converted to light hydrocarbon such as methane (CH_4), ethane (C_2H_6), propane (C_3H_8), etc. The CO_2 hydrogenation was used to determine the overall activity in order to measure the catalytic properties of catalyst sample. The results are shown in Table 5.6. It indicated

that the reaction rate were in the order of Co/Ce-ZrO_2 > 15Co/ZrO_2 > Co-Ce/ZrO_2 >>> 5Ce/ZrO_2. Considering %CO_2 conversion, it also increased in the order of Co/Ce-ZrO_2 > 15Co/ZrO_2 > Co-Ce/ZrO_2 >>> 5Ce/ZrO_2. Considering selectivity to methane, it was found that both Co/Ce-ZrO_2 and Co-Ce/ZrO_2 were similar indicating that the different preparation of both modified-spherical zirconia-supported cobalt catalyst did not affect on methane selectivity.

Table 5.6 Catalytic activities of various catalysts in CO_2 hydrogenation under methanation condition

Sample	Reaction rate ($x10^2$ g CH_2/ g cat· h)	CO_2 conversion % conversion	Product selectivity (%) CH_4	CO
5Ce/ZrO_2	0.74	1.66	92.1	7.7
15Co/ZrO_2	29.7	45.1	98.7	1.3
Co/Ce-ZrO_2	44.1	69.2	98.2	1.8
Co-Ce/ZrO_2	25.4	40.0	97.9	2.1

For 5Ce/ZrO_2, it revealed that the reaction rate and CO_2 conversion was very low indicating low catalytic activities in CO_2 hydrogenation under methanation condition. However, %CO selectivity was the highest. This may be due to the preferable reverse water-gas shift reaction from 5Ce/ZrO_2 catalyst as follows:

$CO_{(g)} + 3\ H_{2(g)} \rightarrow CH_{4(g)} + H_2O_{(v)}$: methanation

$CO_{2(g)} + H_{2(g)} \rightarrow CO_{(g)} + H_2O_{(v)}$: reverse water-gas shift reaction

In comparison between Co/Ce-ZrO_2 and Co-Ce/ZrO_2 with 5Ce/ZrO_2, it was found that Co metal is main catalytic activities in CO_2 hydrogenation under methanation condition of both modified- spherical zirconia-supported cobalt catalyst.

For Co/Ce-ZrO_2, it exhibited the highest catalytic activities in term of reaction rate. This may indicate that Ce metal can improve physical properties of zirconia support resulting in increased catalytic activities. For Co-Ce/ZrO_2, it exhibited catalytic activities in term of reaction rate lower than 15Co/ZrO_2 and those of Co/Ce-ZrO_2. This may indicate that Ce metal adding by the co-impregnation, it may be blocked to the active site of cobalt which made the active cobalt catalyst decreased.

CHAPTER VI

CONCLUSIONS AND RECOMMENDATIONS

In this chapter, section 6.1 provides the conclusions obtained from the experimental results of spherical zirconia supported cobalt catalysts and modified-spherical zirconia-supported cobalt catalyst by adding cerium (Ce) on the spherical zirconia support for CO_2 hydrogenation reaction under methanation condition on characteristics and catalytic properties. Additionally, recommendations for further study are given in section 6.2.

6.1 Conclusions

6.1.1 Characteristics and catalytic properties of spherical zirconia supported cobalt catalysts (Co/ZrO_2), in terms of different cobalt loading

The comparison of characteristics and catalytic performances in CO_2 hydrogenation under methanation condition of a various %wt loading cobalt on the spherical zirconia-supports prepared by the solvolthermal method revealed that cobalt catalysts with 15 wt% and 20 wt% loading have similar properties, such as surface areas, active site molecule, reduction behaviors and % Co dispersion. Both catalysts exhibited high conversion, but the 20 wt% cobalt loading resulted in the highest activity because of probably largest active metals on surface catalyst. It indicated that the amounts of different cobalt metal had distinctive effect on catalytic properties. It was found that the strong interaction between cobalt and zirconia support of all samples was similar.

In addition, in this study, BET results indicated that the spherical zirconia supported has surface area and pore volume that could support the loading of the appropriate 20 wt% of cobalt from this study.

6.1.2 Characteristics and catalytic properties of modified-spherical zirconia supported cobalt catalysts, in terms of different preparation

The comparison of characteristics and catalytic performances in CO_2 hydrogenation under methanation condition of Ce-modified–spherical zirconia-supported cobalt catalysts by different preparation, such as sequential-impregnation (Co/Ce-ZrO_2) and co-impregnation (Co-Ce/ZrO_2) revealed that both catalysts were small size, which were smaller than 5 µm. The physical properties such as surface area, pore volume, pore diameter, good dispersion of metal catalyst of both catalysts were similar. However, the sequential-impregnation (Co/Ce-ZrO_2) exhibited higher %dispersion than that of co-impregnation (Co-Ce/ZrO_2). For the catalytic properties, It showed that the sequential-impregnation (Co/Ce-ZrO_2) exhibited higher activity than that of co-impregnation (Co-Ce/ZrO_2) because of the dispersion of cobalt metal on to ceria-zirconia supports and active site molecule on surface of cobalt catalyst of the sequential-impregnation were higher than that of the co-impregnation.

Cerium (Ce) and Zirconia (ZrO_2) have interaction between both active metals which can improve reducibilities of metal oxide and dispersion of active metals of cobalt catalyst which increased catalytic activities of catalyst. It is clearly shown on preparation by sequential-impregnation (Co/Ce-ZrO_2).

In addition, in this study, Ce metal adding by the co-impregnation, it may be blocked to the active site of cobalt which made the active cobalt catalyst decreased.

6.2 Recommendations

1. Besides ZrO_2 supports, other supports such as Al_2O_3 SiO_2, TiO_2 and MCM-41 and etc should be further investigated with Ce modification.

2. Besides Co metal, other metals such as Ni, Pd and etc should be further investigated with Ce-modification on the supports.

REFERENCES

Aguiar, P., Ram´ırez-Cabrera, E., Laosiripojana, N., Atkinson, A., Kershenbaum, L.S., Chadwick, D. Stud. Surf. Sci. Catal. 145 (2002): 387–390.

Ali, S., Chen, B., and Goodwin Jr., G.R. Zr Promotion of Co/SiO2 for Ficher-Tropsch Synthesis. J. Catal. 157 (1995): 35-41.

Aneggi, E., De Leitenburg, C., Dolcetti, G., Trovarelli, A. Promotional effect of rare earths and transition metals in the combustion of diesel soot over CeO2 and CeO2–ZrO2. Catal. Today 114 (2006): 40-47.

Barrault, J., Guilleminot, A., Achard, J.C., Paul-Boncour, V., and Percheron-Guegan, A. Hydrogenation of carbon monoxide on carbon-supported cobalt rare earth catalysts. Appl. Catal. 21 (1986): 307-312.

Bitter, J.H., Seshan, K., Lercher, J.A. The State of Zirconia Supported Platinum Catalysts for CO_2/CH_4 Reforming. J. Catal. 171 (1997): 279-286.

Borg, Ø., Eri, S., Blekkan, E.A., Storsaeter, S., Wigum, H., Rytter, E., and Holmen, A. Fischer – Tropsch synthesis over γ -alumina-supported cobalt catalysts : Effect of support variables. J. Catal. 248 (2007): 89-100.

Bruce**,** L.A., Hope, G.J., and Mathews, J.F. The activity of cobalt-zirconia and cobalt-nickel-zirconia preparations in the Fischer-Tropsch reaction. Appl. Catal. 8 (1983): 349-358.

Burakorn, T., Panpranot, J., Mekasuwandumrong, O., Chaisuk, C., Praserthdam, P., Jongsomjit, B. Characterization of cobalt dispersed on the mixed nanoscale alumina and zirconia supports. J. Mater. Process. Techno. 206 (2008): 352–358.

Chen, K., Yan, Q. CO hydrogenation over zirconia supported iron catalysts promoted with rare earth oxides. Appl. Catal. A: General 158 (1997): 215-223.

Chuah, G.K. An investigation into the preparation of high surface area zirconia. Catal. Today. 49 (1999): 131-139.

Damyanova, S., Pawalec, B., Arishtirova, K., Maetinez Huerta, M.V., Fierro, J.L.G. Study of the surface and redox properties of ceria-zirconia oxides. Appl. Catal. A 337 (2008): 86-96.

Dow, W.P., Huang, T.J. Effects of Oxygen Vacancy of Yttria-Stabilized Zirconia Support on Carbon Monoxide Oxidation over Copper Catalyst. J. Catal. 147 (1994): 322-332.

Feller, A., Claeys, M. and E.V. Steen, E.V. Cobalt Cluster Effects in Zirconium Promoted Co/SiO_2 Fischer–Tropsch Catalysts. J. Catal. 185 (1999): 120– 130.

Fröhlich, G., Kestel, U., Łojewska, J., Łojewski, T., Meyer, G., Voß, M., Borgmann, D., Dziembaj. R., and Wedler, G. Activation and deactivation of cobalt catalysts in the hydrogenation of carbon dioxide. Appl. Catal. A: General 134 (1996): 1-19.

Guerrero-Ruiz, A., Sepu´lveda-Escribano and Rodri´guez-Ramos, I. Carbon monoxide hydrogenation over carbon supported cobalt or ruthenium catalysts. promoting effects of magnesium, vanadium and cerium oxides. Appl. Catal. A 120 (1994): 71-83.

Iglesia, E. Design, synthesis, and use of cobalt-based Fischer-Tropsch synthesis catalysts. Appl. Catal. A. 161 (1997): 59-78.

Jongsomjit, B., Panpranot, J., and Goodwin. Jr., J.G. Effect of zirconia-modified alumina on the properties of Co/γ -Al2O3 catalysts. J. Catal. 215 (2003): 66–77.

Khaodee, W., Jongsomjit, B., Praserthdam, P., Goto, S., Assabumrungrat, S. Impact of temperature ramping rate during calcination on characteristics of nano-ZrO2 and its catalytic activity for isosynthesis. J. Mol. Catal. A: Chem. 280 (2008): 35-42.

Kraum, M., and Baerns, M. Fischer–Tropsch synthesis: the influence of various cobalt compounds applied in the preparation of supported cobalt catalysts on their performance. Appl. Catal. A. 186 (1999): 189–200.

Lahtinen, J., Anraku, T., Somorjai, G.A. CO and CO hydrogenation on cobalt foil model catalysts: evidence for the need of CoO reduction. Catal. Lett. 25 (1994): 241-255.

Li, X., Asami, K., Luo, M., Michiki, K., Tsubaki, N., Fujimoto, K. Direct synthesis of middle iso-paraffins from synthesis gas. Catal. Today 84 (2003): 59–65.

Mattos, L.V., Rodino, E., Resasco, D.E., Passos, F.B., Noronha, F.B. Partial oxidation and CO_2 reforming of methane on Pt/Al_2O_3, Pt/ZrO_2, and $Pt/Ce–ZrO_2$ catalysts. Fuel Process. Technol. 83 (2003): 147–161.

Mercera, P.D.L., Van Ommen, J.G., Doesburg, E.B.M., Burggraaf, A.J., Ross, J.R.H. Zirconia as a support for catalysts Influence of additives on the thermal stability of the porous texture of monoclinic zirconia. J. Appl. Catal. 71 (1991): 363-391.

Milt, V.G., Spretz, R., Ulla, M.A., Lombardo, E.A. Zirconia-Supported Cobalt as a Catalyst for Methane Combustion. J. Catal. 200 (2001): 241-249.

Nagaoka, K., Okamura, M., Aika, K. Titania supported ruthenium as a coking-resistant catalyst for high pressure dry reforming of methane. Catal. Commun. 2 (2001): 255–260.

Osendi, M.I., Moya, J.S., Serna, C.J., Soria, J. Metastability of Tetragonal Zirconia Powders. J. Am. Ceram. Soc. 68 (1985): 135-139.

Özkara-Aydınoğlu, Ş., Özensoy, E., Aksoylu, A.E. Carbon dioxide reforming of methane over Co-X/ZrO_2 catalysts (X=La, Ce, Mn, Mg, K). Catal. Commun. 11 (2010): 1165-1170.

Özkara-Aydınoğlu, Ş., Özensoy, E., Aksoylu, A.E. The effect of impregnation strategy on methane dry reforming activity of Ce promoted Pt/ZrO_2. Int. J. Hydrogen Energy 34 (2009): 9711–9722.

Panpranot, J., Taochaiyaphum, N., Jongsomjit, B., Praserthdam, P. Differences in characteristics and catalytic properties of Co catalysts supported on micron- and nano-sized zirconia. Catal. Commun. 7 (2006): 192-197.

Pérez-Alonso, F.J., Ojeda, M., Herranz, T., Rojas, S., González-Carballo, J.M., Terreros, P., Fierro, J.L.G. Carbon dioxide hydrogenation over Fe–Ce catalysts. Catal. Commun. 9 (2008): 1945-1948.

Riva, R., Miessner, H., Vitali, R., Piero, G.D. Metal–support interaction in Co/SiO_2 and Co/TiO_2. Appl. Catal. A 196 (2000): 111–123.

Stagg-Williams, S.M., Noronha, F.B., Fendley, G., Resasco, D.E. CO_2 Reforming of CH_4 over Pt/ZrO_2 Catalysts Promoted with La and Ce Oxides. J. Catal. 194 (2000): 240–249.

Sun, S., Tsubaki, N., Fujimoto, K. The reaction performances and characterization of Fischer–Tropsch synthesis Co/SiO_2 catalysts prepared from mixed cobalt salts. Appl. Catal. A 202 (2000): 121–131.

Tani, E., Yoshimura, M., Somiya, S. Formation of Ultrafine Tetragonal ZrO_2 Powder Under Hydrothermal Conditions. J. Am. Ceram. Soc. 66 (1983): 11-14.

Valmor, R., Mastelaro, Valérie Briois, Dulcina P. F. de Souza and Carlos L. Silva. Structural studies of a ZrO_2–CeO_2 doped system. J. Eur. Ceram. Soc. 23 (2003): 273-282.

Wang, H.Y., Ruckenstein, E. Carbon dioxide reforming of methane to synthesis gas over supported rhodium catalysts: the effect of support. Appl. Catal. A 204 (2000): 143–152.

Wongmaneenil, P., Jongsomjit, B., Praserthdam, P. Solvent effect on synthesis of zirconia support for tungstated zirconia catalysts. J. Ind. Eng. Chem. 16 (2010): 327-333.

Zhang, Y.,Wei, D., Hammache, S., Goodwin. Jr., G.J. Effect of Water Vapor on the reduction of Ru-Promoted Co/Al2O3. J. Catal. 188 (1999): 281–290.

APPENDICES

APPENDIX A

CALCULATION FOR CATALYST PREPARATION

Preparation of spherical zirconia supported, ZrO_2

Zirconium dioxide was prepared by solvothermal reaction. Approximately, 35 g of zirconium tetra-n-butoxide 80 wt% solution in 1-butanol (ZNB, Aldrich) was suspended in 100 ml of the desired solvent in a test tube, which was then placed in a 300 ml autoclave. The solvent used in this work was 1,4-butanediol (purity 99%, Sigma–Aldrich). The gap between autoclave wall and the test tube was filled with 30 ml of the same solvent. The autoclave was completely sealed and purged with nitrogen. The mixture was heated to 300^0C at a heating rate of 2.5^0C/min and kept at that temperature for 2 h. After cooling to room temperature, the resulting powders were collected after repeated washing with methanol by centrifugation. The products were then air-dried at 110^0C for 12 h and calcined at 450^0C for 3 h at a heating rate of 10^0C/min.

After finished above procedure, will get the spherical zirconia supported that already

Calculation of cobalt loading

Preparation of 20%wt Co/ZrO_2 by the incipient wetness impregnation method was shown as follow:

Reagent: - Cobalt (II) nitrate hexahydrate ($Co(NO_3)_2 \cdot 6H_2O$)

Molecular weight = 291.03 g/mol

Cobalt (Co), Atomic weight = 58.933 g/mol

- Support: the spherical zirconia supported

Based on 1.00 g of catalyst used, the composition of the catalyst would be as follows:

Cobalt = 0.20 g

ZrO_2 = 1.00 – 0.20 = 0.80 g

Cobalt 0.20 g was prepared from Cobalt (II) nitrate hexahydrate

Cobalt (II) nitrate hexahydrate required = $\frac{0.20}{58.933}$ x 291.03

= 0.9877 g

Calculation of cerium loading

Preparation of 5%wt Ce/ZrO_2 by the incipient wetness impregnation method was shown as follow:

Reagent: - Cerium(III) nitrate hexahydrate ($Ce(NO_3)_3 \cdot 6H_2O$)

Molecular weight = 434.226 g/mol

Cerium (Ce), Atomic weight = 140.12 g/mol

- Support: the spherical zirconia supported

Based on 1.00 g of catalyst used, the composition of the catalyst would be as follows:

Cerium = 0.05 g

ZrO_2 = 1.00 – 0.05 = 0.95 g

Cobalt 0.05 g was prepared from Cerium(III) nitrate hexahydrate

Cerium(III) nitrate hexahydrate required = $\frac{0.05}{140.12}$ x 434.226

= 0.1549 g

APPENDIX B

CALCULATION FOR TOTAL CO CHEMISORPTION AND DISPERSION

Calculation of the total CO chemisorption and metal dispersion of the catalyst, a stoischiometry of CO/Co = 1, is assumed. The calculation procedure is as follows:

Let the weight of catalyst used	=	W	g
Integral area of CO peak after adsorption	=	A	unit
Integral area of 100 µl of standard H_2 peak	=	B	unit
Amounts of CO adsorbed on catalyst	=	B-A	unit
Concentration of Co	=	C	%wt
Volume of H_2 adsorbed on catalyst	=	100 × [(B-A)/B]	µl
Volume of 1 mole of CO at 30 °C	=	24.86 x 10^6	µl

Mole of CO adsorbed on catalyst = [(B-A)/B]×[100/24.86] µmole

Total CO chemisorption = [(B-A)/B]×[100/24.86]×[1/W] µmole /$g_{catalyst}$

= N µmole /$g_{catalyst}$

$$\%Co\ dispersion = \frac{\text{The amount of cobalt equivalent to CO adsorption after reduction} \times 100}{\text{Total amount of cobalt active sites expected to exist after reduction}}$$

Molecular weight of cobalt = 58.93

Metal dispersion (%) = $\dfrac{1 \times CO_{tot} \times 100}{\text{No. µmole Co}_{tot}}$

= $\dfrac{1 \times N \times 100}{No.\ \mu mole\ Co_{tot}}$

= $\dfrac{1 \times N \times 58.93 \times 100 \times 100}{\left[C \times 10^6\right]}$

= $\dfrac{0.59 \times N}{C}$

APPENDIX C

CALCULATION FOR REDUCIBILITY

For supported cobalt catalyst, it can be assumed that the major species of calcined Co catalysts is Co_3O_4. H_2 consumption to reduce Co_3O_4 is calculated as follows:

Molecular weight of Co = 58.93

Molecular weight of Co_3O_4 = 240.79

Calculation of the calibration of H_2 consumption using cobalt oxide (Co_3O_4)

Let the weight of Co_3O_4 used = 0.1 g

= 4.153×10^{-4} mole

From equation of Co_3O_4 reduction;

$$Co_3O_4 + 4H_2 \rightarrow 3Co + 4H_2O \qquad (E.1)$$

Mole of hydrogen consumption = 4 Mole of Co_3O_4 consumption

= $4\times4.153\times10^{-4}$

= 1.661×10^{-3} mole

Integral area of hydrogen used to reduce Co_3O_4 0.1 g = 115.63 unit

At 100 % reducibility, the amount of hydrogen consumption is 1.661×10^{-3} mole related to the integral area of Co_3O_4 after reduction 115.63 unit.

Calculation of reducibility of supported cobalt catalyst

$$\%\,\text{Reducibility} = \frac{\text{Amount of } H_2 \text{ uptake to reduce 1 g of catalyst} \times 100}{\text{Amount of theoretical } H_2 \text{ uptake to reduce } Co_3O_4 \text{ to } Co^0 \text{ for 1 g of catalyst}}$$

Integral area of the calcined catalyst = X unit

The amount of H_2 consumption = $\left[2\times1.661\times10^{-3}\times(X)/115.63\right]$mole

Let the weight of calcined catalyst used = W g

Concentration of Co = Y %wt

Mole of Co = $\left[(\mathrm{W}\times\mathrm{Y}/100)/58.93\right]$ mole

Mole of Co_3O_4 = $\left[(\mathrm{W}\times\mathrm{Y}/100)/(3\times58.93)\right]$ mole

Amount of theoretical = $\left[(\mathrm{W}\times\mathrm{Y}/100)\times4/(3\times58.93)\right]$mole

Reducibility (%) of supported Co catalyst = $\dfrac{\left[2\times1.661\times10^{-3}\times(X)/115.63\right]\times100}{\left[(W\times Y/100)\times4/(3\times58.93)\right]}$

Example for 20Co/ Z

Integral area of the calcined catalyst = *4.574 unit*

The amount of H_2 consumption = $\left[2\times1.661\times10^{-3}\times(X)/115.63\right]$*mole*

Let the weight of calcined catalyst used = *0.0589 g*

Concentration of Co = *20 %wt*

Mole of Co = $\left[(0.0589\times20/100)/58.93\right]$*mole*

Mole of Co_3O_4 = $\left[(0.0589\times20/100)/(3\times58.93)\right]$ *mole*

Amount of theoretical = $\left[(0.0589\times20/100)\times4/(3\times58.93)\right]$*mole*

Reducibility (%) of supported Co catalyst $= \dfrac{\left[2\times1.661\times10^{-3}\times(4.574)/115.63\right]\times100}{\left[(0.0589\times20/100)\times4/(3\times58.93)\right]}$

= 49.3 %

APPENDIX D

CALIBRATION CURVES

This appendix showed the calibration curves for calculation of composition of reactant and products in CO_2 hydrogenation reaction. The reactant is CO_2 and the main product is methane. The other products are linear hydrocarbons of heavier molecular weight that are C_2-C_4 such as ethane, ethylene, propane, propylene and butane.

The thermal conductivity detector, gas chromatography Shimadzu model 8A was used to analyze the concentration of CO by using Molecular sieve 5A column.

The VZ10 column are used with a gas chromatography equipped with a flame ionization detector, Shimadzu model 14B, to analyze the concentration of products including of methane, ethane, ethylene, propane, propylene and butane. Conditions uses in both GC are illustrated in Table C.1.

Mole of reagent in y-axis and area reported by gas chromatography in x-axis are exhibited in the curves. The calibration curves of CO_2, CO, methane, ethane, ethylene, propane, propylene and butane are illustrated in the following figures.

Table D.1 Conditions use in Shimadzu modal GC-8A and GC-14B.

Parameters	Condition	
	Shimadzu GC-8A	Shimadzu GC-14B
Width	5	5
Slope	50	50
Drift	0	0
Min. area	10	10
T.DBL	0	0
Stop time	50	60
Atten	0	0
Speed	2	2
Method	41	41
Format	1	1
SPL.WT	100	100
IS.WT	1	1

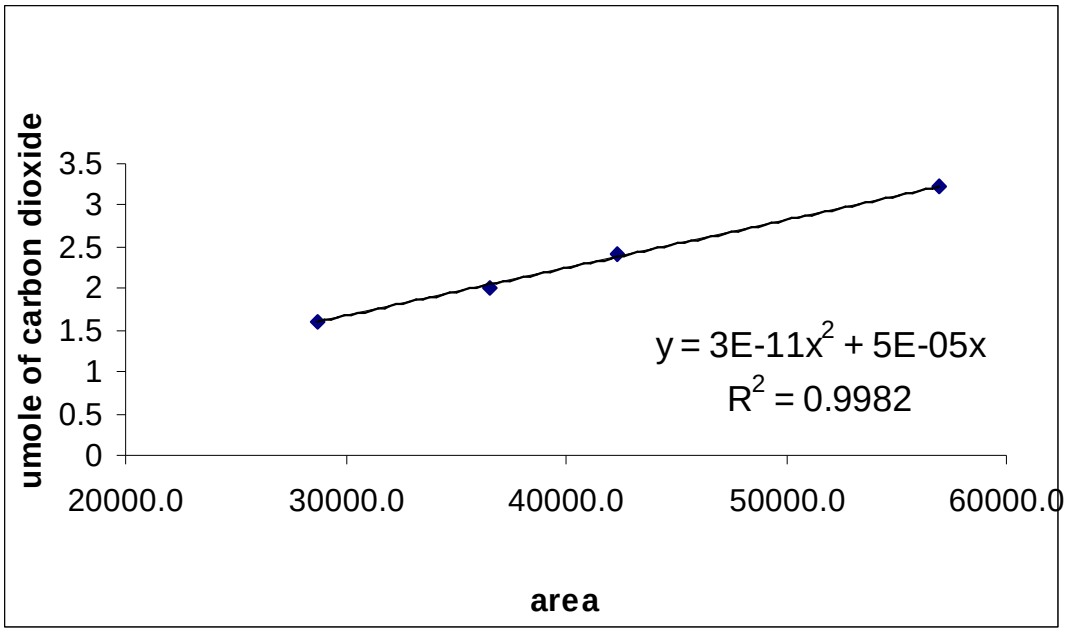

Figure D.1 The calibration curve of carbon dioxide (CO_2).

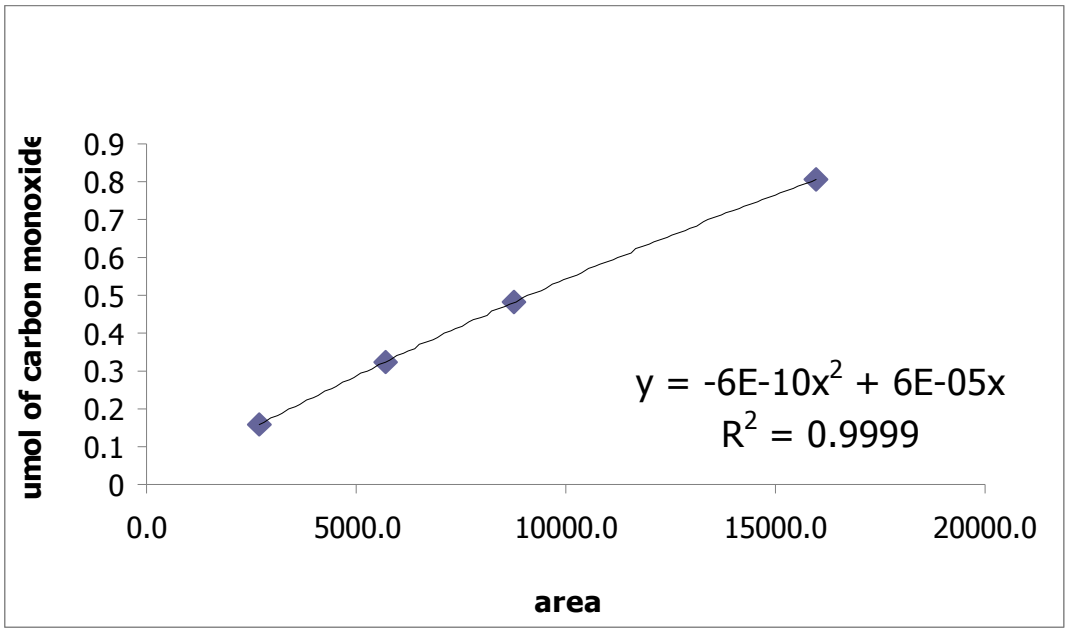

Figure D.2 The calibration curve of carbon monoxide (CO).

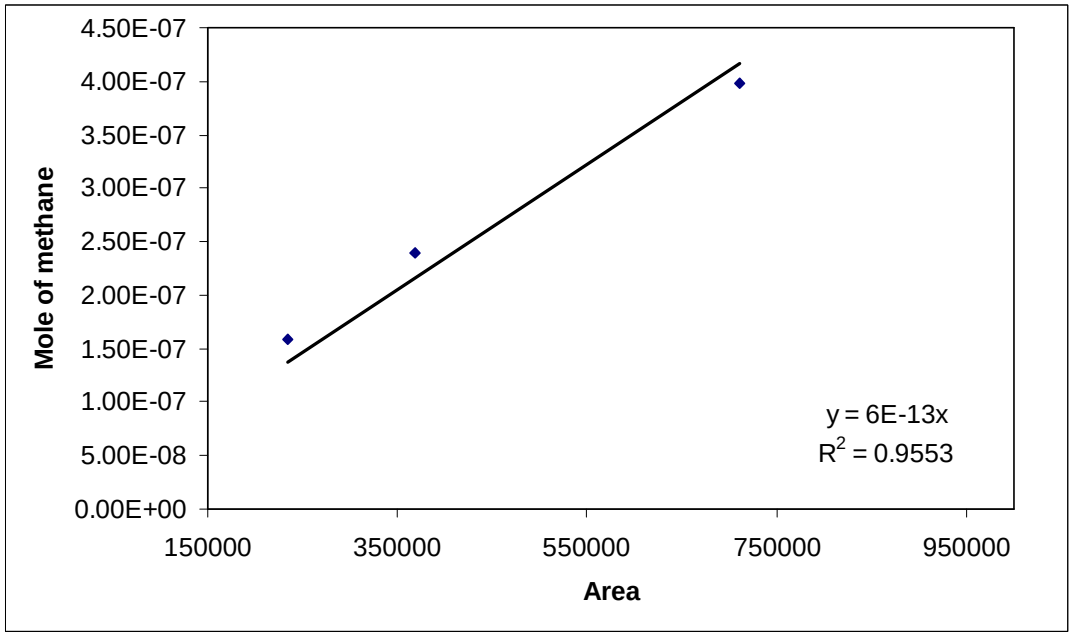

Figure D.3 The calibration curve of methane.

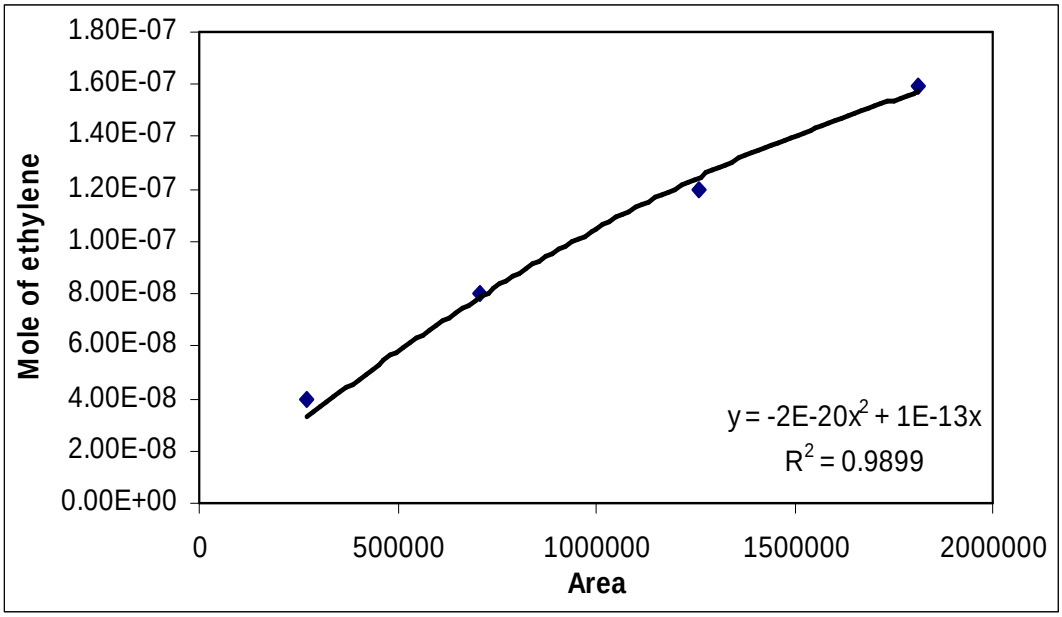

Figure D.4 The calibration curve of ethylene.

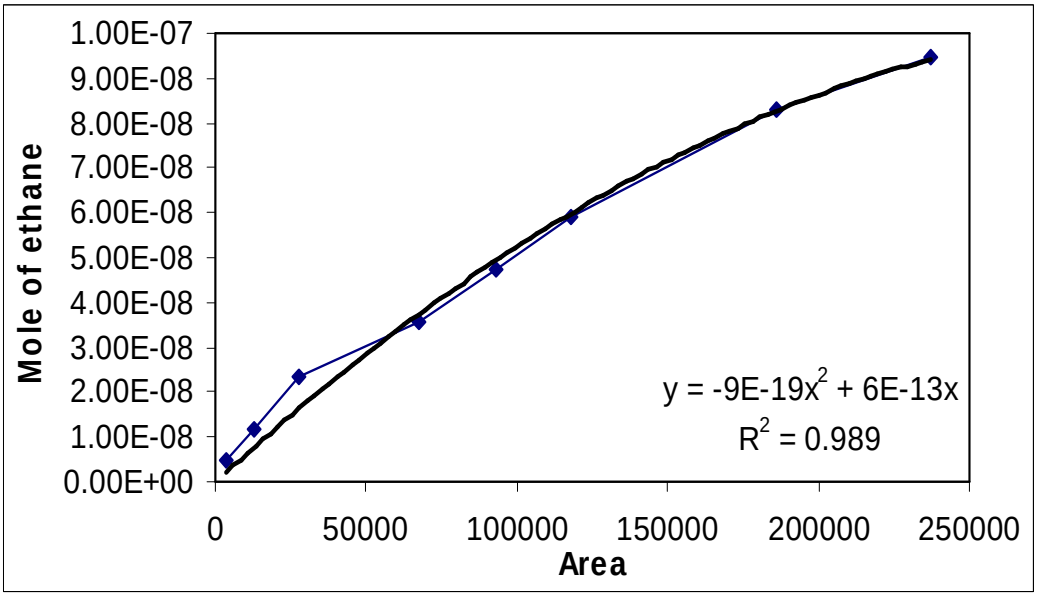

Figure D.5 The calibration curve of ethane.

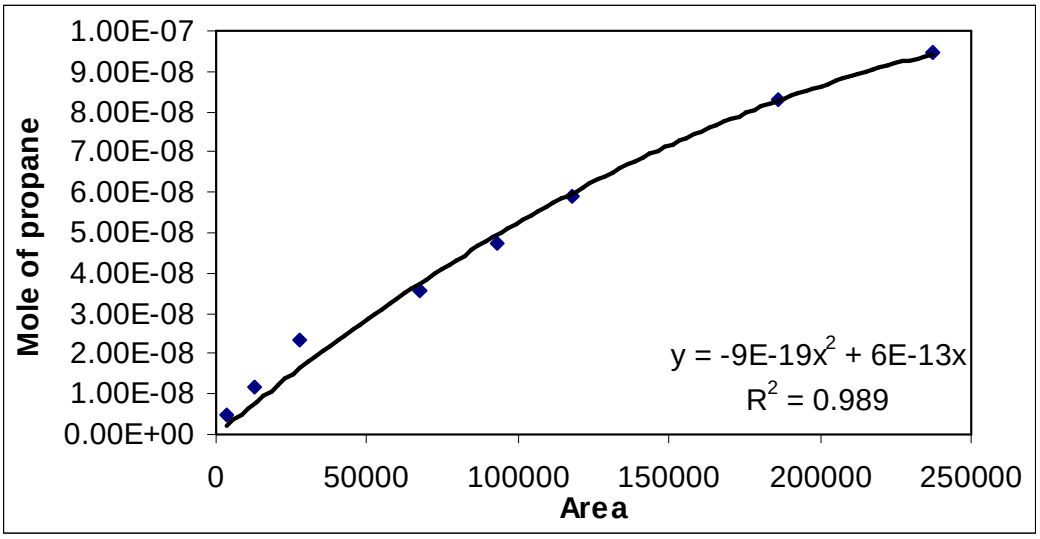

Figure D.6 The calibration curve of propane.

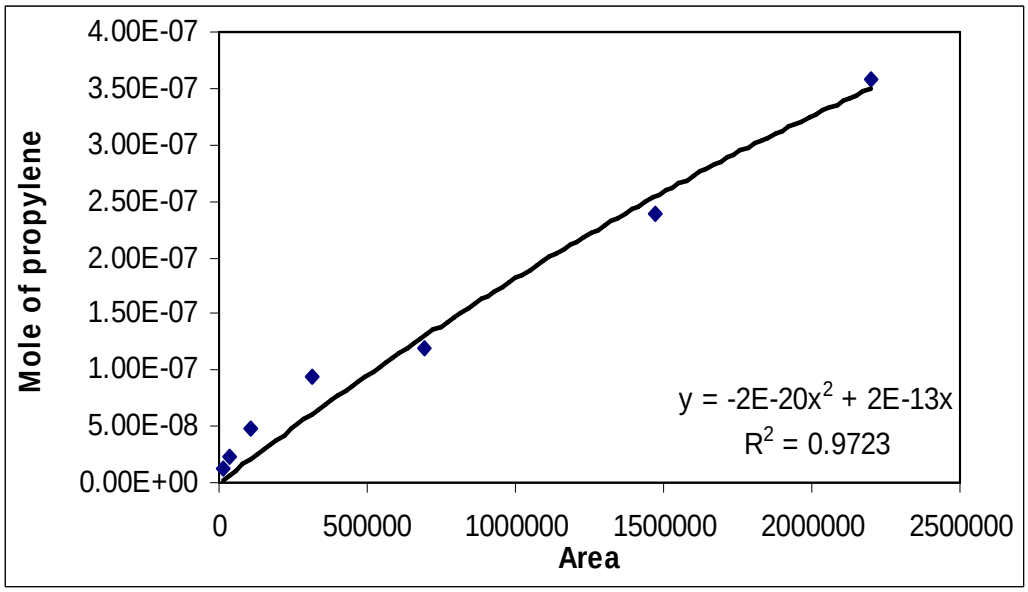

Figure D.7 The calibration curve of propylene.

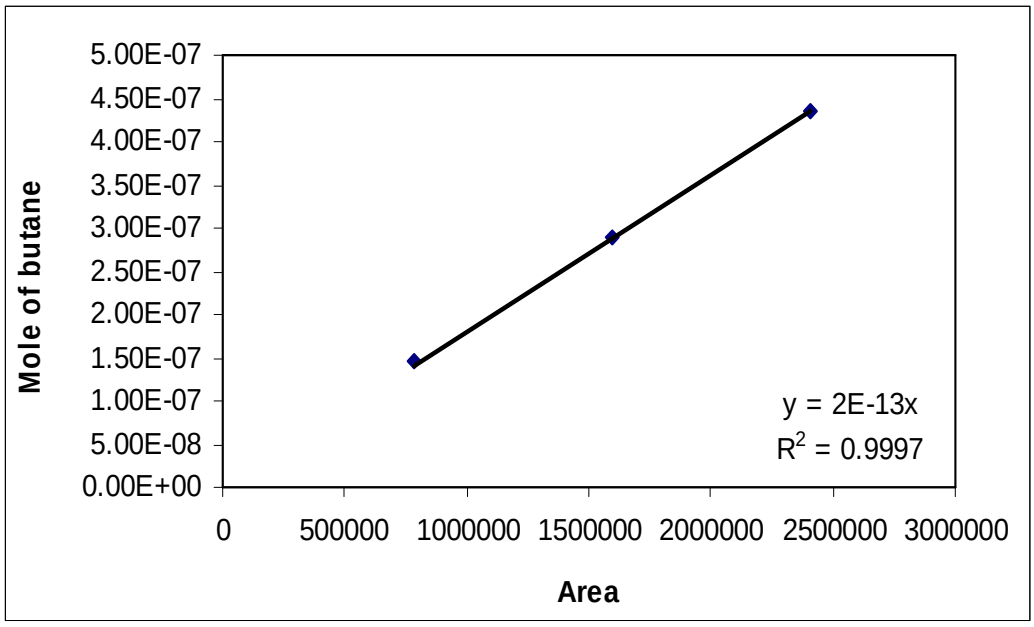

Figure D.8 The calibration curve of butane.

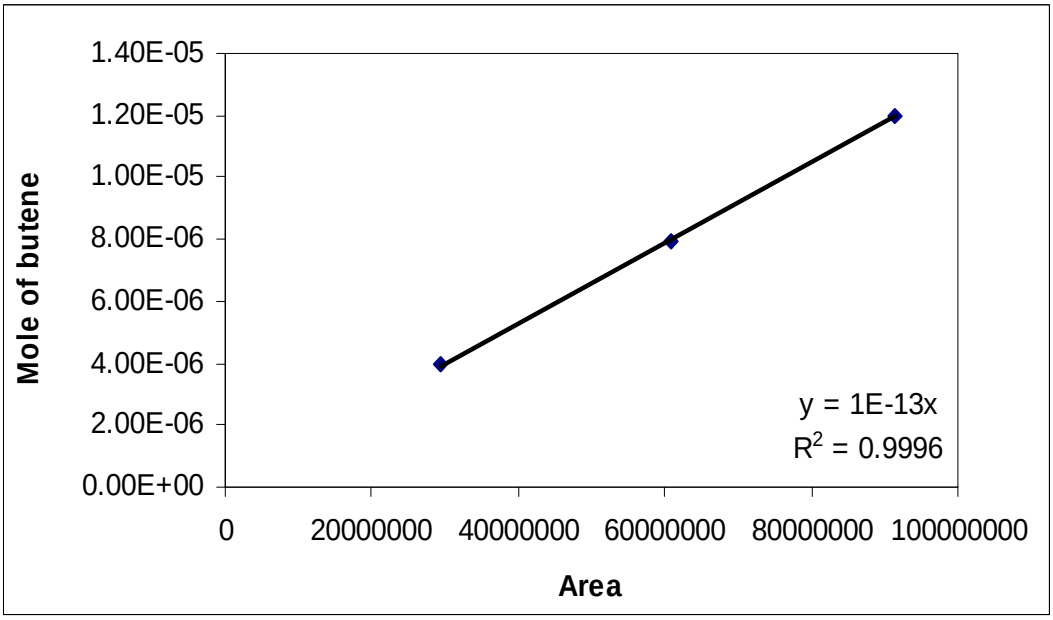

Figure D.9 The calibration curve of butene.

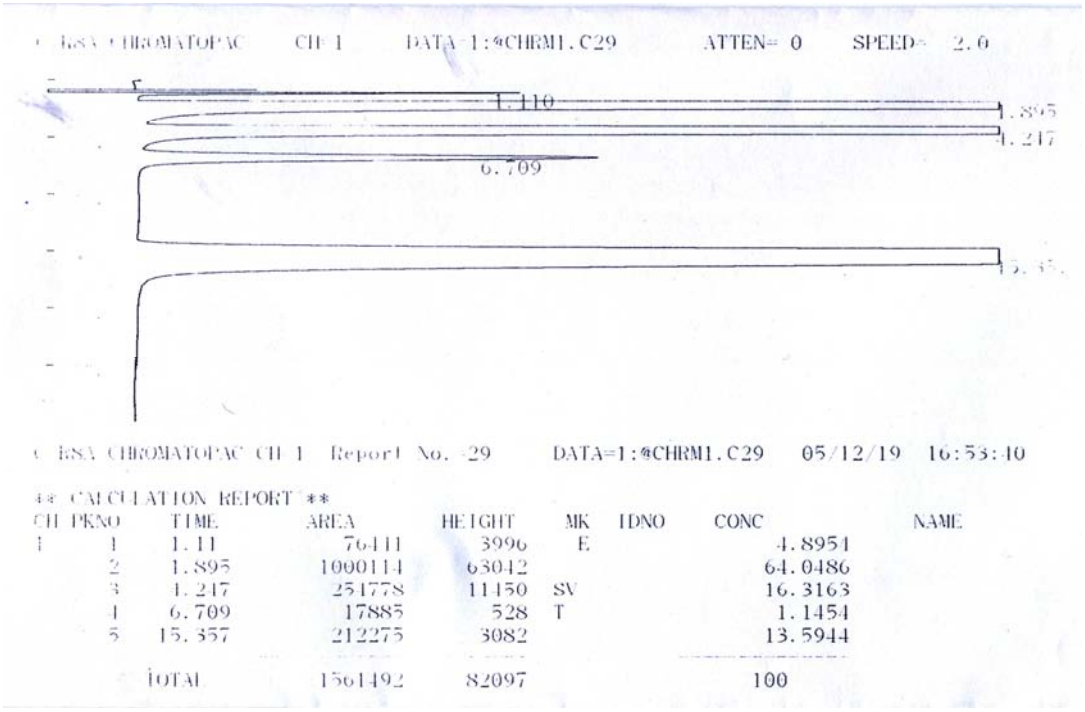

Figure D.10 The chromatograms of catalyst sample from thermal conductivity detector, gas chromatography Shimadzu model 8A (Molecular sieve 5A column).

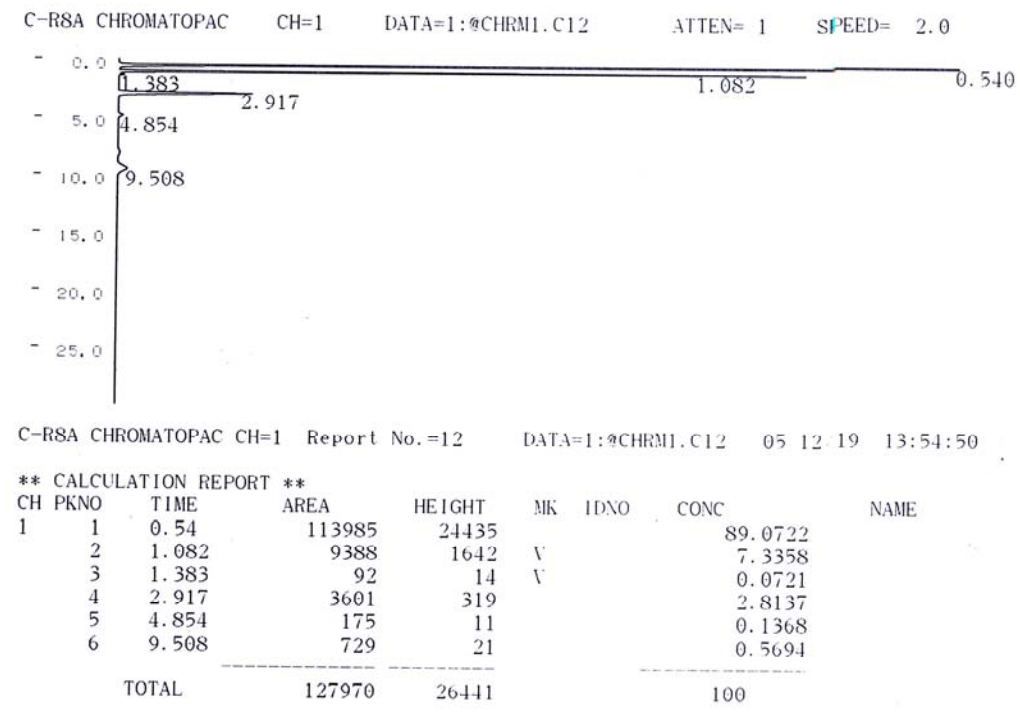

Figure D.11 The chromatograms of catalyst sample from flame ionization detector, gas chromatography Shimadzu model 14B (VZ10 column).

APPENDIX E

CALCULATION OF CO_2 CONVERSION, REACTION RATE AND SELECTIVITY

The catalyst performance for the CO_2 hydrogenation was evaluated in term of activity for CO_2 conversion, reaction rate and selectivity.

CO_2 conversion is defined as moles of CO_2 converted with respect to CO_2 in feed:

$$CO_2 \text{ conversion (\%)} = \frac{100 \times [mole\,of\ CO_2\ in\ feed - mole\,of\ CO_2\ in\ product]}{mole\,of\ CO_2\ in\ feed} \quad \text{(i)}$$

Reaction rate was calculated from CO_2 conversion that is as follows:

Let the weight of catalyst used	=	W	g
Flow rate of CO_2	=	2	cc/min
Reaction time	=	60	min
Weight of CH_2	=	14	g
Volume of 1 mole of gas at 1 atm	=	22400	cc
Selectivity to CH_4	=	S	

$$\text{Reaction rate (g } CH_2\text{/g of catalyst.h)} = \frac{(\%\ conversion\,of\ CO_2\ /100) \times 60 \times 14 \times 2}{W \times 22400} \times S \quad \text{(ii)}$$

Selectivity of product is defined as mole of product (B) formed with respect to mole of CO_2 converted:

$$\text{Selectivity of B (\%)} = 100 \times [mole\,of\ B\ formed\ /\ mole\,of\ total\ products] \quad \text{(iii)}$$

Where B is product, mole of B can be measured employing the calibration curve of products such as methane, ethane, ethylene, propane, propylene and butane

mole of CH_4 = (area of CH_4 peak from integrator plot on GC-14B) x 8 x 10^{12} (iv)

VITA

Mr. Wittaya Hewararak was born on 10nd April 1982, in Nakhonsithammarat, Thailand. He finished high school from Satree Thungsong School, Nakhonsithammarat, in 2000, and graduated Bachelor degree of Chemical Engineering from Faculty of Engineering, Prince of Songkla University, Songkla, Thailand, in March 2004. After finished bachelor degree, He has been worked at IRPC public company limited in process engineering section. After he worked 6 years, He decided to continued Master's study at the Department of Chemical Engineering, Faculty of Engineering, Chulalongkorn University in 2009. He study master's degree and worked at IRPC together.